EFFECTS OF FILLERS ON MORPHOLOGICAL, MECHANICAL, FLOW AND THERMAL PROPERTIES OF BITUMINOUS COMPOSITES

A THESIS SUBMITTED TO
THE GRADUATE SCHOOL OF NATURAL AND APPLIED SCIENCES
OF
MIDDLE EAST TECHNICAL UNIVERSITY

BY

ÜMİT TAYFUN

IN PARTIAL FULFILLMENT OF THE REQUIREMENTS
FOR
THE DEGREE OF MASTER OF SCIENCE
IN
POLYMER SCIENCE AND TECHNOLOGY

DECEMBER 2006

Approval of Graduate School of Natural and Applied Sciences

_____

Prof. Dr. Canan Özgen
Director

I certify that this thesis satisfies all the requirements as a thesis for degree of Master of Science.

_____

Assoc. Prof. Göknur Bayram
Head of the Department

This is to certify that we have read this thesis and that in our opinion it is fully adequate, in scope and quality, as a thesis for the degree of Master of Science.

_____

Prof. Dr. Erdal Bayramlı
Supervisor

Examining Committee Members

Assoc. Prof. Göknur Bayram	(METU, CHE)	_____
Prof. Dr. Erdal Bayramlı	(METU, CHEM)	_____
Prof. Dr. Nesrin Hasırcı	(METU, CHEM)	_____
Prof. Dr. Teoman Tinçer	(METU, CHEM)	_____
Prof. Dr. Ali Usanmaz	(METU, CHEM)	_____

I hereby declare that all information in this document has been obtained and presented in accordance with academic rules and ethical conduct. I also declare that, as required by these rules and conduct, I have fully cited and referenced all material and results that are not original to this work.

Name, Last name: Ümit Tayfun

Signature

ABSTRACT

EFFECTS OF FILLERS ON MORPHOLOGICAL, MECHANICAL, FLOW AND THERMAL PROPERTIES OF BITUMINOUS COMPOSITES

Tayfun, Ümit
M.S., Department of Polymer Science and Technology
Supervisor: Prof. Dr. Erdal Bayramlı

December 2006, 88 pages

There are many different types of fillers used for bitumen modification such as; silica, limestone, basalt, mica, oyster shells. Filler gives rigidity, stiffness or hardness, regulates thermal expansion and shrinkage, improves heat resistance, and modifies rheological properties of bituminous composites.

The main objective of this study was to determine the effect of filler type and ratio on mechanical, thermal properties and morphologies of bitumen based composites. It was also aimed to improve the heat resistivity of the bituminous composite to obtain a material with good mechanical and heat isolation properties.

Bituminous composites were prepared by using Brabender Plasti-Corder, PLV 151. Mixing was made at 180 ºC with 60 rpm for 15 minutes. Two grades of bitumen as 20/30 and 50/70 penetrations were used. $CaCO_3$, CaO, mica, baryte, kieselguhr and silaned kieselguhr were used as fillers in this study. Ethylene vinyl acetate copolymer,

styrene–butadiene rubber, and styrene–butadiene–styrene block copolymer were used as polymers.

According to the test results, using mica at low percentages had the effect of decreasing the viscosity of the bitumen due to its flow alignment property. Baryte gave high heat capacity and low heat conductivity to bituminous material. EVA containing samples showed the best combination on mechanical properties. The silanation process decreased the pore sizes as observed in mercury porosimetry experiments. A decreased amount of bitumen impregnation was obtained by the silanation process, clearly observed in SEM micrographs.

Keywords: Bitumen, bituminous composites, filler, porosity, silane treatment

ÖZ

DOLGU MALZEMELERİNİN BİTÜMLÜ KOMPOZİTLERİN MORFOLOJİK, MEKANİK, AKIŞ VE ISISAL ÖZELLİKLERİNE ETKİSİ

Tayfun, Ümit
Yüksek Lisans, Polimer Bilimi ve Teknolojisi Bölümü
Tez Danışmanı: Prof. Dr. Erdal Bayramlı

Aralık 2006, 88 Sayfa

Silika, kireç, bazalt, mika, istridye kabukları gibi birçok farklı dolgu malzemesi bitüm modifikasyonu için kullanılmıştır. Dolgu malzemesi bitümlü kompozite esnemezlik, katılık veya sertlik verir, ısısal genleşmesini ve çekmesini düzenler, ısıl dayanımını artırır, reolojik özelliklerini modifiye eder.

Bu çalışmanın temel amacı; dolgu malzemesi cinsi ve oranının bitüm bazlı kompozitlerin mekanik, ısıl özelliklerine ve morfolojisine etkisini belirlemektir. Aynı zamanda iyi mekanik ve ısıl yalıtım özellikli bir malzeme elde etmek için bitümlü kompozitin ısıl dayanımını iyileştirmek amaçlanmıştır.

Bitümlü kompozitler Brabender Plasti-Corder, PLV 151 kullanılarak hazırlanmıştır. Karıştırma 15 dakika boyunca 60 devir/dakika ile 180 ºC de yapılmıştır. 20/30 ve 50/70

penetrasyonluk iki tip bitüm kullanılmıştır. $CaCO_3$, CaO, mika, barit, kieselguhr ve silanlanmış kieselguhr bu çalışmada dolgu malzemeleri olarak kullanılmıştır. Polimerler olarak etilen vinil asetat kopolimeri, stiren–bütadiyen kauçuğu ve stiren-bütadiyen-stiren kopolimeri kullanılmıştır.

Test sonuçlarına göre; düşük yüzdelerde mika kullanımının, akış doğrultusunda yönlenme özelliğinden dolayı bitümün viskozitesini azaltma etkisi vardır. Barit bitümlü malzemeye yüksek ısı kapasitesi ve düşük ısıl iletkenlik vermektedir. EVA içeren örneklerin mekanik özellikleri diğerleri ile karşılaştırıldığında daha iyi olduğu gözlemlenmiştir. Silanlama işlemi, civalı porozimetre deneylerinde gözlendiği üzere boşluk boyutlarını azaltmıştır. Silanlama işlemi ile elde edilen azalan bitüm emilimi miktarı SEM mikrofotoğrafları ile açıkça gözlemlenmiştir.

Anahtar Kelimeler: Bitümen, bitümlü kompozitler, dolgu malzemesi, porozite, silanlama işlemi

Dedicated to my family

ACKNOWLEDGEMENTS

I would like to express my deepest gratitude to my supervisor Prof. Dr. Erdal Bayramlı, for his continuous support, encouragement and guidance throughout this study.

I am very grateful to Prof. Dr. Teoman Tinçer from Department of Chemistry for giving me every opportunity to use the instruments in his laboratory.

Special thanks go to Cengiz Tan from Department of Metallurgical and Materials Engineering for SEM Analysis and Osman Yaslıtaş from Department of Chemistry for his thecnical support.

I wish to thank sincerely Mehmet Doğan who was always beside me with his friendship and brotherhood.

I express my special thanks to Güral Özkoç for his friendly and helpful contributions during my studies. I wish to thank also my friends Ümit Hakan Yıldız, Selahattin Erdoğan, Yasin Kanbur, Ali Sinan Dike, and Fuat Çankaya.

Last but not the least; I wish to express my sincere thanks to my family for supporting, encouraging, and loving me all through my life.

TABLE OF CONTENTS

LIST OF TABLES

TABLES

LIST OF FIGURES

FIGURES

CHAPTER I

INTRODUCTION

Bitumen is a general term for a group of materials composed of mixtures of hydrocarbons that are fusible and soluble in carbon disulfide. Included in the group are petroleum, asphalts, asphaltites, and mineral waxes [1]. Bituminous materials are primary engineering materials which function largely because they are highly water resistant and thermoplastic. Because they are complex organic materials which have a "structure," and because they can be highly variable, understanding of their composition, behavior and utilization has required much study in many fields in the attempted conversions from an art to the principles of fundamental science. Rheology and physical chemistry especially have been importance [2].

A mineral filler is an inorganic additive which, when mixed with a bitumen, retains its original size and shape, does not react with the bitumen, and does not assume colloidal properties in the filler-bitumen mixture. Mineral fillers in bituminous composition have a history as old as that of bitumens themselves. More than 5000 years ago, the naturally occurring bitumens used as waterproofings and brick-laying mortars contained contaminants that acted as fillers. During the early 1900's, manufacturers and users of bituminous materials began to appreciate the value of mineral fillers and to understand their function in varying capacities for controlling and improving the physical properties of bituminous products. Today mineral fillers are used extensively to fulfill a multitude of important functions [2].

In this study, it was aimed to investigate the effects of fillers on the mechanical, rheological, and thermal properties of polymer-modified bituminous materials. Materials were prepared by using counter-rotating internal mixer. Two different

bitumen grades; 20/30 penetration bitumen and 50/70 penetration bitumen were used. $CaCO_3$ was used as main filler almost for all of the samples. CaO, Baryte, Mica, Kieselguhr and silaned kieselguhr are the fillers which were used separately with different concentrations. Surface silanated kieselguhr was prepared by mixing kieselguhr with silicone oil in acetone solution for an hour. It was aimed to get materials which pores inside kieselguhr stay unfilled with the help of surface silanation process.

Several thermoplastics and elastomers have been mixed with bitumen, usually in proportions below 10%, to improve the properties of the binder. Ethylene vinyl acetate (EVA) copolymer have revealed as good modifiers to improve permanent deformation and thermal cracking. Elastomers, like styrene–butadiene rubber (SBR) and styrene–butadiene–styrene block copolymer (SBS) are very suitable, because besides of improving mechanical properties ageing is also upgraded [3]. In this work, Styrene Butadiene Styrene Block Copolymer (SBS), Ethylene Vinyl Acetate (EVA) and Styrene Butyl Rubber (SBR) were used as polymers.

For characterization of the samples, Scanning Electron Microscopy (SEM) was utilized to observe the dispersions of fillers inside the materials. Mechanical behavior of the prepared samples was investigated by performing tensile test. Melt Flow Index (MFI) measurements were done to examine the effects of different fillers on flow properties of the bituminous materials. Thermal properties of samples were observed with thermal conductivity measurements by using Hot Wire Method.

CHAPTER 2

BACKGROUND INFORMATION

2.1 Bitumen

2.1.1 Definition of Bitumen

Bitumen and asphalt are both generic terms. In USA, the word asphalt is used as synonymous with bitumen- the refinery product which has now largely replaced the natural asphalts that occur in Trinidad, Venezuela, Cuba etc. Outside USA however, the word asphalt is generally taken to mean a mixture of refinery bitumen with a substantial proportion of solid mineral matter [4].

Bitumen is a generic term referring to flammable, brown or black mixtures of tarlike hydrocarbons, derived naturally or by distillation from petroleum. It can be in the form of a viscous oil to a brittle solid, including asphalt, tars, and natural mineral waxes. Substances containing bitumens are called bituminous, e.g., bituminous coal, tar, or pitch [5].

Bitumen is a semi-solid material which can be produced from certain crude oils by distillation. It can also be found in nature as "natural asphalt". It is a mixture of four main components–aromatics, paraffins, asphaltenes and resins [3].

At room temperature bitumen is a flexible material with a density of 1 g/cm^3, but at low temperatures it becomes brittle and at high temperatures it flows like a viscous liquid. The physical, mechanical and rheological properties of the bitumen depend

basically on its colloidal structure, linked to the chemical composition, in particular to the proportion of asphaltenes and maltenes [3].

2.1.2 Chemical Composition of Bitumen

Bitumen is made up of polar and non-polar compounds in complex association. The interaction of polar compounds determines bitumen structure and mechanical properties [6].

The chemistry of the bitumen produced depends on two main parameters, the crude source and the manufacturing process. The crude source is most influential for processes that involve no chemical modification of the final bitumen blend. In such systems the bitumen may be optimized for properties but not improved on. For systems where a chemical modification of the bitumen can be carried out or components from other feed sources can be introduced unsatisfactory bitumen may be made satisfactory [2].

Bitumen can be conveniently viewed on two levels, the molecular and the inter-molecular. The molecular is important to determine the potential for structure formation and the inter-molecular for the types of structuring that exist [2].

The knowledge of bitumen chemistry is very scant and is largely based on separation by means of organic solvents into groups of similiar properties. For asphaltic bitumens, Marcusson gave the following groups of compounds whose nomencalture is generally accepted. Carboids represent that part of the asphaltic bitumen which is insoluble in carbon bisulfide. Carbenes are soluble in carbon bisulfide but insoluble carbon tetrachloride. The carboids and carbenes are present in very small quantities only and are therefore of minor importance [2].

Asphalts are colloidal dispersions of very high molecular weight hydrocarbons called asphaltenes (dispersed phase) in a dispersion medium called maltenes. Asphaltenes are agglomerates of the most polar molecules in the bitumen and this polarity is derived from the hetero-atoms namely sulfur, oxygen and nitrogen. Maltenes are the

dispersion oil medium of lesser aromaticity and consist of two fractions namely oils and resins. Oils are the liquid portion of the bitumen containing mormal, iso and cyclo paraffins and condensed naphthenes with some alkyl aromatics. Resins are transition chemical compounds between oils and asphaltenes, and they are chemically very similar to asphaltenes but with lesser polar characteristics [7].

The concentration of asphaltenes, their particle size and the nature of dispersed phase and dispersion medium are the key aspects, which determines asphalt properties and behaviour. On review of the basic aspects of bitumen chemistry, it is precise to conclude that bitumen is made up of polar and non-polar compounds in a complex association. Hence, the bitumen chemistry depends on two main aspects namely crude source and the manufacturing process. By properly choosing the feedstocks and processing conditions, it is possible to produce high performance bitumen with correct balance in chemical composition, molecular weight distribution and physical characteristics [7].

Control of the chemical composition of the bitumen by restricting choice of crudes and manufacturing schemes has become increasingly difficult. Nowadays, the refiners tend to use variety of crudes for processing and large amounts of residues and heavy ends from unconventional routes are also blended into short residues for processing into bitumen. In a complex refinery with lube manufacturing facilities, heavy extracts and hard pitch from propane deasphalting units and other heavy waste oils have to be processed with short residue in Biturox reactor. Hence, additive systems are being adopted increasingly all over the world to affect proper balance in chemical composition of bitumen thereby changing its rheology and improving resistance to thermal deformation, mechanical and elastic behaviour [7].

Bitumen quality varies with the variation in crude oil source and the processing scheme, causing considerable difficulty in improving its performance characteristics. Rheological properties of bitumen depend largely on asphaltene content [7].

At constant temperature, the viscosity of the bitumen increases as the concentration of asphaltenes dispersed in maltenes is increased. However with asphaltene content and saturate/resin ratio remaining constant, the increased aromatic content does not have any effect on the rheology of bitumen other than marginal reduction in shear susceptibility [7].

Resin present in bitumen tends to harden it by increasing its viscosity value while the penetration index and shear stability decreases. The structure and molecular weight of paraffin waxes present in bitumen makes it poorer in quality. At low temperature conditions, pavements exhibit signs of distress in the form of fine cracks, if waxes are high in the bitumen binder. Also, waxes act as a flux at high temperature and paved bitumen starts bleeding, exhibiting its high temperature susceptibility [7].

Elemental analysis is an averaging, it gives little information on molecular arrangements and so sheds little light on physical properties. Bitumens do contain trace amounts of metals, mainly vanadium and nickel. Table 2.1 shows several asphalts that give an indication of the range observed in elemental analysis [2].

Table 2.1 Elemental analysis of bitumen

Element (wt%)	Mexican	Arkansas	Boscan	Calif
Carbon	83.77	85.78	82.90	86.77
Hydrogen	9.91	10.19	10.45	10.94
Nitrogen	0.28	0.26	0.78	1.10
Sulphur	5.25	3.41	5.43	0.99
Oxygen	0.77	0.36	0.29	0.20
Vanadium	180 ppm	7 ppm	1380 ppm	4 ppm
Nickel	22 ppm	0.4 ppm	109 ppm	6 ppm

Although all asphalts are predominantly carbon and hydrogen most of the molecules contain at least one heteroatom (S, N, 0). The heteroatoms are often present in sufficient amounts such that on average every molecule has one. These may be in the rings, in non ring components or as functional groups attached to compounds. These together with polarisable aromatic rings contribute polarity [2].

It is the arrangement of different elements/atoms, into molecules that determines the interactions of these molecules and hence the physical properties. Because the heteroatoms often impart functionality and polarity they have a disproportionate effect on the properties. This includes effects such as aging, the more reactive the hetero atoms age faster (e.g. sulfur) [8].

2.1.3 Uses of bitumen

The use of bitumen is perhaps one of the world's oldest crafts and has a history spanning 5,000 years. The ancient Egyptians were particularly adept at handling the murky material mummifying their dead with bandages coated in natural pitch.

Nowadays, most of the bitumen used is produced as a by-product of crude oil refinery although natural bitumen is still used for special applications.

Consumption has grown to 75 million tonnes a year with road construction grabbing the lion's share (80%). The bitumen is combined with crushed rock known as aggregate to form asphalt for road paving. Much of the rest is used for roofing, insulation and waterproofing [9].

For many years well over 80% of world consumption of bitumen, which is estimated at 100 million tonnes, has been used for paving applications, the construction and maintenance of roads. The rest is used for various purposes. The use of bitumen in road maintenance can be up to four times its use in road construction [2].

The use of bitumen in industry accounts for less, than 20% of world bitumen production. It is nevertheless important to those manufacturers and engineers who rely on its particular properties as an economical binder and protector. In many parts of the world it is used extensively to waterproof the roofs of houses, often in the form of shingles which are strips of felt first impregnated with bitumen and then covered on both sides with harder bitumen and a coating of mineral granules. A similar construction technique involves sheets of bitumensaturated felt laid onto a flat roof with layers of bitumen below, between and above them. In more complex roofing projects, bitumen is to be found holding in place a protective coating of chippings on the cantilevered roof of a sports stadium. By contrast, bitumen is also used in dampproofing and floor composition tiles [2].

Other materials, particularly felts and papers, are impregnated with bitumen to improve their performance as regards insulation. Packaging papers, printing inks, linoleum, sound deadening felts hidden inside car bodies and the undersealing compounds beneath them, electrical insulating compounds and battery boxes are some of the hundreds of industrial and domestic products likely to contain bitumen [2].

2.2 Polymer

2.2.1 The aim of using polymers with bitumen

Modification of natural bitumen with synthetic polymers constitutes a route to overcome the new technical demands. Several thermoplastics and elastomers have been mixed with bitumen, usually in proportions below 10%, to improve the properties of the binder employed in roads. Polyethylene and ethylene vinyl acetate EVA copolymer have revealed as good modifiers to improve permanent deformation and thermal cracking. Polypropylene fibers are also used, especially to ameliorate cracking. Elastomers, like styrene–butadiene rubber (SBR) and styrene–butadiene–styrene block copolymer (SBS) are very suitable, because besides of improving

mechanical properties ageing is also upgraded. Recently, the case of blends of bitumen with recycled polymers has been considered, with the advantage of disposing troublesome waste plastics.

The major concern of bitumen/polymer blends is their lack of stability during prolonged storage at high temperatures. The tendency to phase separation under quiescent conditions appears as an important limitation for the practical use of these blends. The stability is affected by polymer particle size and shape, since phase separation is caused by coalescence and subsequent creaming [3].

2.2.2 Interaction between bitumen and polymer

Structural and chemical changes have been observed during the mixing process of polymers and bitumen. Various factors such as chemical compatibility, polymer chemical nature, molecular weight, particle size, bitumen nature, as well as blending process conditions such as type of mixing/dispersing device, time and temperature play important role in determining the modified asphalt properties [10].

Synthetic elastomers, such as styrene-butadiene-styrene (SBS) and styrene-butadiene-rubber (SBR), are common and very effective polymer modifiers. SBS modified bitumens show two phase morphology at microscopic level. The modified bitumen with a low SBS content exhibit a continuous bitumen phase in which the polymer particles are dispersed. On the other hand, the modified bitumens with a high SBS content exhibit a polymeric continuous phase in which bitumens globules are dispersed [11].

EVA is also used as polymeric modifier in bituminous materials. At low polymer content, small polymer droplets swollen by bitumen light fractions appear in a continuous bitumen phase. By increasing the polymer concentration, continuous polymer phase appear [12].

Polymers are much larger molecules than bitumen so they can have a dramatic effect on bitumen film properties. Polymers will:

- increase the softening point: the flow point is higher and so susceptibility to bleeding is decreased.
- increase the binder viscosity: the resistance to flow is higher at any given temperature so film thickness can be higher with subsequent improved aging resistance.
- decrease the thermal susceptibility: the binder has higher stiffness at high temperature and lower stiffness at low temperature that is its properties are much more uniform with temperature.
- increase the elastomer properties: the ability to absorb energy and elongate with stress and recover after stress is removed. Leads to improved deformation and crack resistance.
- increase cohesion: Improved strength to resist fracture.
- increase low temperature tensile strength and flexibility: Leads to better low temperature crack resistance and less likelihood of brittle fracture at low temperatures [13].

2.3. Fillers

From the earliest days man has dug out of the ground many of his raw materials and in the course of time has put them to a vast range of uses. Without the variety of these natural resources and the realisation of their potential today's modern civilisation could not exist [13].

Fillers, as the name implies, have commonly been employed to cheapen or extend a product with an evident change or modification of the properties of the unfilled materials such as hardness, rigidity, viscosity or colour. Gradually, the realisation grew that by the selective use of fillers, certain properties of the unfilled material

could be enhanced or even exceeded and a 'reinforcement' of properties was possible. Hence fillers are today employed to obtain any, or a combination, of the following effects:

1. add rigidity, stiffness or hardness.
2. regulate thermal expansion and shrinkage.
3. improve heat resistance.
4. improve or regulate electrical characteristics.
5. increase strength and reduce creep.
6. modify rheological properties (thixotropy, 'body').
7. aid processability (lubrication, mixing, dispersion, etc.).
8. modify appearance (opacity, colour, texture).
9. alter density and bulk.
10. lower cost.

The scientific evaluation of pulvarized minerals involves first a consideration of their primary properties, such as particle size, size distribution, particle shape and surface configuration or texture, and then the relation of these to the secondary properties of powder, namely, surface area, packing of the particles and void content, and average void size in the compacted powder. These secondary properties can, in turn, be related to the consistency and flow characteristics of the filled asphalt [13].

2.3.1 Effects of Fillers to Bituminous Materials

When mineral powders are used as fillers for asphalt the chemical nature of the mineral should be considered. Asphalts which by nature are slightly acidic show better adherence to alkaline than to acidic surfaces. Also, the age and history (weathering) of the mineral surface has considerable effect on its reaction towards asphalt. Any filler with some chemical affinity for asphalt tends to disperse in hot asphalt or cutbacks. Mineral powders which are not readily wetted by asphalt tend to agglomerate and are difficult to disperse in the liquid. The use of additives to improve

dispersion may be effective but frequently is not economical. Surface texture (roughness) aids in the adherence of asphalt to a solid but this effect should not be confused with the bonding which is dependent on chemical forces [13].

For most practical uses asphalts are blended with some kind of pulvarized mineral to increase consistency of the binder. In an asphalt road the material in the aggregate, which is less than 74 microns in diameter, may be considered the binder for the larger pieces of aggregate comprising the paving mixture. In reality, the chief function of the fine powder present in a bituminous mixture is to increase the viscosity of the asphalt. The same result could be obtained by using a harder asphalt, but this would result in the sacrifice of longer serviceability to be expected from the softer asphalt used with the filler [13].

2.3.2 Carbonates

The next most abundant naturally occurring element to silicon is calcium, which is found mainly as calcium carbonate, the principal constituent of chalk, limestone and marble. These materials have been largely derived from the consolidation of deposits of minute marine organisms (foraminifera, coccoliths, etc.) during the formation of the earth's crust. Chalk deposits have resulted from soft compression, limestone rocks from hard compression and finally metamorphism has given marble [14].

Calcium carbonate occurs naturally in two crystalline forms, calcite and aragonite, the former being the more stable and abundant form. Calcite is rhombohedral, has a specific gravity of 2.71 and a hardness of 3.0 moh. Aragonite is the orthorhombic form and occurs naturally as needle-shaped prisms or spherulites in thermal springs. It has a specific gravity of 2.93 and a hardness of 3.5 moh. When heated aragonite is transformed into calcite [14].

The production of calcium carbonate minerals is by open quarrying of the massive rock into pieces small enough to be crushed, followed by mechanical crushing and

grading of the broken stone. The final stage is fine grinding by roll and ball milling, jet milling or micronising [14].

High purity whiting (99,75 % $CaC0_3$) of regulated particle shape and size and degree of aggregation is obtained by chemical precipitation methods. Limestone is first calcined in kilns, then drawn off and slaked to give calcium hydroxide. The hydroxide is purified and made into slurry through which is passed purified carbon dioxide obtained from the calcining stage. The precipitation stage is carefully controlled to obtain fine uniform particles. The best white and lighter whitings are, however, obtained by the precipitation of calcium carbonate from calcium chloride solution by the addition of sodium carbonate solution or ammonium carbonate. Lightness is achieved by using dilute solutions at a low temperature. From both methods the precipitate is washed, collected and dried [14].

Figure 2.1 SEM photograph of calcium carbonate [14]

Precipitated calcium carbonate consists of a mixture of calcite and aragonite as illustrated in Figure 2.2, in proportions which vary according to the method of manufacture. The product from the calcium chloride processes has a particle size ranging from 0.05 μm (ultrafine grades) up to 10 μm. The particles have a cubical shape typical of the calcite crystal. The milk of lime process produces calcium

carbonate having needle-like crystals typical of aragonite and an average partide size of 0.5 μm [14].

2.3.3 Barium Sulphate (Baryte)

Barytes or heavy spar ($BaS0_4$) is the chief natural source of barium sulphate which is frequently found in association with metallic sulphate ores often occurring as well developed orthorhombic crystals resembling calcite. Baryte has a density of 4.4 g/ml The mineral is converted to the sulphide by calcination with coal or coke and then to the chloride by treatment with hydrochloric acid. Sodium sulphate is added and blanc fixe or precipitated barium sulphate is formed. Blanc fixe is also a by-product in the manufacture of hydrogen peroxide. The natural barium sulphates of selected particle size distribution are used as fillers in polyurethane foams to impart high density, higher load bearing properties and improved processing. Barium sulphate is obtained in dry ground or water ground grades as off-white or white powders [14].

Table 2.2 General properties of Barytes [14]

Property	Barytes	
	Wet ground	Dry ground
Particle Size, max	20μm	60 μm
Particle Size, av.	3 μm	12 μm
Passing 325 mesh. sieve	99.99%	99.95%
Oil Absorption	8-9	5-6

The difference in properties of the two grades is shown in Table 2.2. Apart from their use in polymers as a low bulking high density chemically resistant filler, plastics containing it are opaque to X-rays [14].

2.3.4. Mica

The substitution of an atom of aluminium for silicon in pyrophyllite and the introduction of a potassium atom leads to the formula for potash mica (muscovite or white mica) $K.Al_2(Si_3Al)O_{10}.(OH)_2$. The potassium atom bridges adjacent silica layers so that their distance apart is constant and characteristic of all micas. Similarly, starting with talc and performing the same substitution, magnesium mica orphlogopite $[K.Mg_3(Si_3Al)O_{10}.(OH)_2]$ is obtained. Numerous other substitutions are found with sodium, calcium, lithium and iron. All micas are characterised by an excellent basal cleavage through the weak potassium linkages which enables the natural silica layers to be split into very thin sheets less than $25x10^{-6}$ m thick. The sheets are flexible and elastic through a very wide angle and possess excellent dielectric strength and a low thermal conductivity. Dry or wet ground mica is used mostly in thermosetting resins to improve electrical properties and heat resistance. Mica is dimensionally stable, moisture resistant and difficult to wet with resins. The latter factor and its basic cost limit its use as filler in polymers to materials for electrical resistance applications [14].

2.3.5. Diatomaceous Earth (DE)

Alternatively called Kieselguhr, Tripoli or Infusorial Earth according to its place of origin and nature, diatomaceous earth is a form of opaline silica consisting of the fossilised remains of immense deposits of diatoms, i.e. unicellular free swimming plants belonging to the large group of algae. Diatomite is a loosely pulvemlent material with an earthy texture [14]. It is a sedimentary rock compose of the skeletal remains of diatoms which sedimented 15 million years ago during the middle and upper Miocene period. The organic material of diatoms decomposed, and rain water washed it out and purified the diatoms, leaving almost pure silica of very porous

structure (porosity from 65 to 85%) characterized by a system of numerous channels encapsulated in a perferated shell. One can easily predict that material having such high a porosity is able to absorb high amounts of liquids. Their oil absorption varies in the range of 100-200g/100g [15]. Since it is composed of the hollow shells of diatoms it absorbs four to fivetimes its own weight of water [14]. Particle size varies in the range of 1-20 μm, depending on the method of processing, which includes disintegration, air classification, and sometimes calcination. The pH ranges between 7 and 10, whereas the moisture content is from 0.5 to 6.0 %, but most of this moisture is bonded with only 0.2% of water, reactive with the system [15]. It possesses good heat, electrical and sound insulating properties and is also thermally and chemically resistant. Hydrated silica constitutes 70-90 % of the material, the rest consists of impurities in the form of sand, iron hydroxides, clayes, calcareuos and organic matter. The pure white variety is dug from open pits and dried in the open or in sheds and calcined. The impurer forms are washed and purified by sedimentation processes and the iron contaminants removed by acid treatment [14].

Tripoli or tripolite is a more compact laminate form, geologically older than kieselguhr. It has a density of 1.86 and it is porous. Diatomaceous earth is used in resins to improve their heat resistance and electrical properties giving a compound of lower density than that given by mica or asbestos. The filler is abrasive and can cause damage to mould surfaces [14]. High water absorption and effect on gloss and sheen are the main reasons for their application as flatting agents in paints [15].

The most notable character of the shells inside the kieselguhr is that they are permeated by pores forming a delicate lace like structure which gives diatomite its unique properties. The pores in the shells are very small (1-3 μm) in diameter and often many species have an even finer network of secondary pores (<0.5 μm) within the primary pores (Figure 2.2). The diatom shells and fragments can range in size from 1-1000 μm, however the average size is between 50-100 μm depending on species and growth conditions. Depending on species the shape of the shells can also vary, but are frequently boat shaped or wheel like in appearance [16].

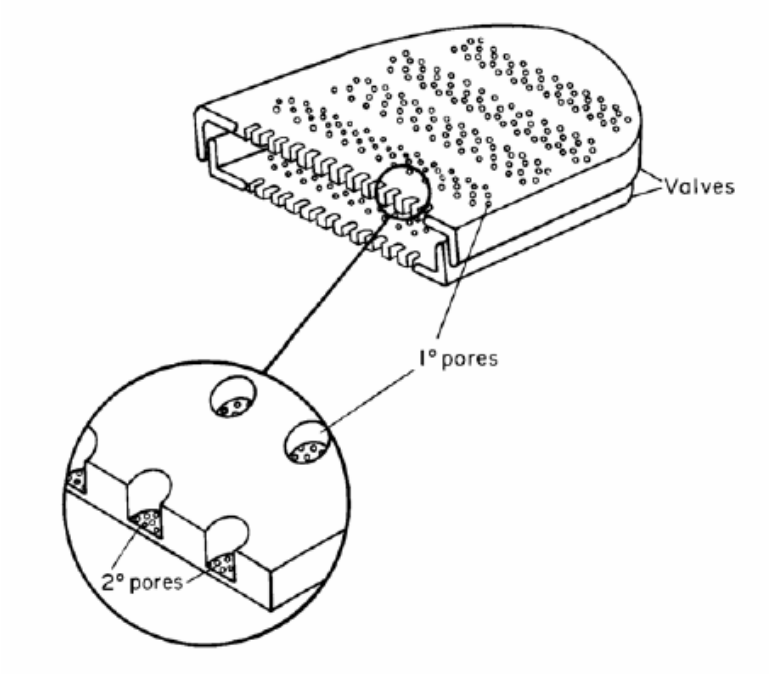

Figure 2.2 Detailed wiew of diatom shell [16]

Figure 2.3 shows an example of a diatomaceous earth deposit. The skeletons are composed of opal-like, amorphous silica ($SiO_2(H_2O)_x$) having a wide range of porous, fine structures. The natural grades are uncalcinated powders classified according to particle size distribution. During the calcination process, the moisture (~40% in DE) is also removed due to the high process temperature, which may also cause sintering of DE partides to dusters [17].

Figure 2.3 An example of a DE deposit with a single principal diatom present, x1OOO [16]

2.4 Mechanical Properties

There are a variety of methods which are useful in predicting mechanical properties of polymers. However, it is essential that there should be some consistency in the manner in which tests are conducted, and in the interpretation of their results. This consistency is accomplished by using standardized testing techniques. Establishment and publication of these standards are often coordinated by professional societies. In the United States the most active organization is the American Society for Testing and Materials (ASTM). Its annual book of ASTM standards comprises numerous volumes, which are issued and updated yearly; a large number of these standards relate to mechanical testing techniques [18].

2.4.1 Tensile Tests

Tensile elongation and tensile modulus measurements are among the most important indications of strength in a material and are the most widely specified properties of plastic materials. Tensile test, in a broad sense, is a measurement of the ability of a material to withstand forces that tend to pull it apart and to determine to what extent the material stretches before breaking. Tensile modulus,

an indication of the relative stiffness of a material, can be determined from a stress-strain diagram. Different types of plastic materials are often compared on the basis of tensile strength, elongation, and tensile modulus data. Many plastics are very sensitive to the rate of straining and environmental conditions. Therefore, the data obtained by this method cannot be considered valid for applications involving load-time scales or environments widely different from this method. The tensile property data are more useful in preferential selection of a particular type of plastic from a large group of plastic materials and such data are of limited use in actual design of the product. This is because the test does not take into account the time-dependent behavior of plastic materials [18].

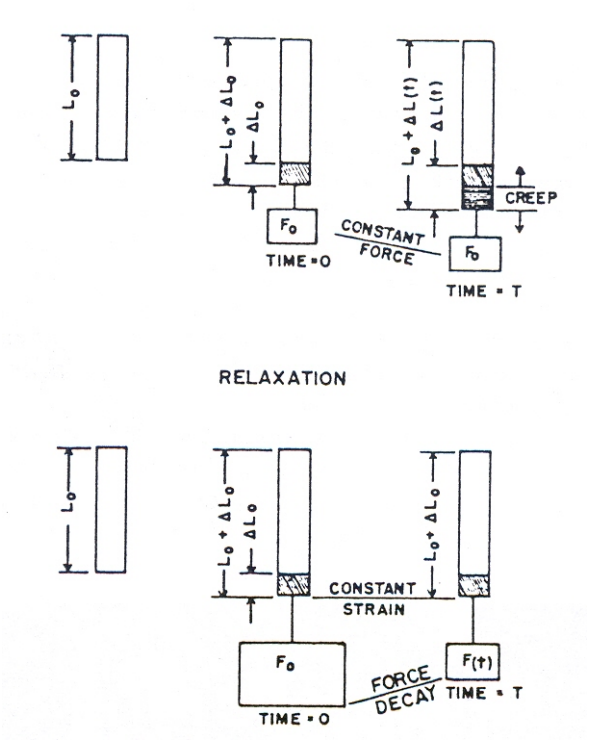

Figure 2.4 Diagram illustratrating creep and stress relaxation [18]

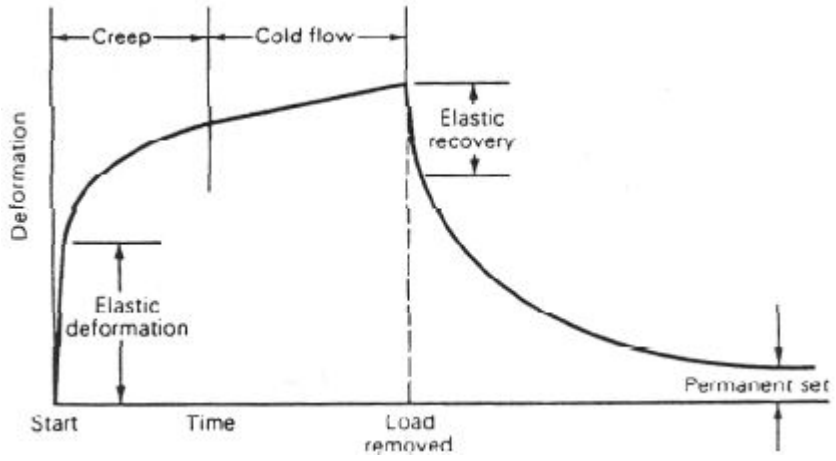

Figure 2.5 Diagram illustrating creep and cold flow [18]

The tensile testing machine of a constant-rate-of-crosshead movement is used. It has a fixed or essentially stationary member carrying one grip, and a movable member carrying a second grip. Self-aligning grips employed for holding the test specimen between the fixed member and the movable member prevent alignment problems. A controlled-velocity drive mechanism is used. Some of the commercially available machines use a closed-loop servo-controlled drive mechanism to provide a high degree of speed accuracy. A load-indicating mechanism capable of indicating total tensile load with an accuracy of 1 percent of the indicated value or better is used. Lately, the inclination is toward using digital-type load indicators which are easier to read than the analog-type indicator so, an extension indicator, commonly known as the extensometer, is used to determine the distance between two designated points located within the gauge length of the test specimen as the specimen is stretched. The advent of new microprocessor technology has virtually eliminated time-consuming manual calculations. Stress, elongation, modulus, energy, and statistical calculations are performed automatically and presented on a visual display or hard copy printout at the end of the test. Creep and stress relaxation effects are shown in Figure 2.4, creep and cold flow behavior of plastics are illustrated in Figure 2.5 [18].

Test specimens for tensile tests are peepared many different ways. Most often, they are either injection molded or compression molded. Figure 2.6 shows ASTM D 638 Type I tensile test specimen most commonly used for testing rigid and semirigid plastics. Since the tensile properties of some plastics change rapidly with small changes in temperature, it is recommended that tests be conducted in the standard laboratory atmosphere of 23 ± 2°C and 50 ± 5 percent relative humidity [18].

2.4.1.1 Tensile Strength

The speed of testing is the relative rate of motion of the grips or test fixtures during the test. There are basically five different testing speeds specified in the ASTM D 638 Standard. The most frequently employed speed of testing is 0.2 in/min whenever possible; the speed indicated by the specification for the material being tested should be used. If a test speed is not given, appropriate speed that causes rupture between 30 sec and 5 min should be chosen [18].

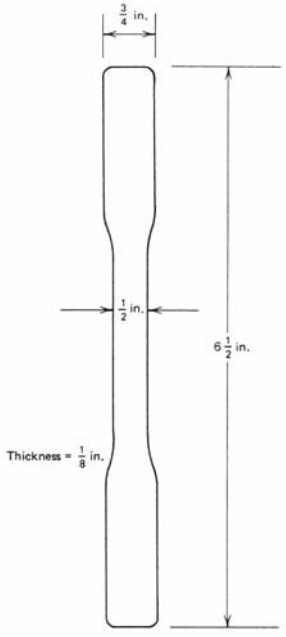

Figure 2.6 Tensile test specimen (Type 1) [18]

The test specimen is positioned vertically in the grips of the testing machine. The grips are tightened evenly and firmly to prevent any slippage. The speed of testing is set at the proper rate and the machine is started. As the specimen elongates the resistance of the specimen increases and is detected by a load cell. This load value (force) is recorded by the instrument. Some machines also record the maximum (peak) load obtained by the specimen, which can be recalled after the completion of the test. The elongation of the specimen is continued until a rupture of the specimen is observed. Load value at break is also recorded. The tensile strength at yield and at break (ultimate tensile strength) is calculated [18].

$$\text{Tensile strength} = \frac{\text{Force (Load) (N)}}{\text{Cross section area } (mm^2)} \qquad (1)$$

$$\text{Tensile strength at yield (MPa)} = \frac{\text{Maximum load recorded (N)}}{\text{Cross section area } (mm^2)} \qquad (2)$$

$$\text{Tensile strength at break (MPa)} = \frac{\text{Load recorded at break (N)}}{\text{Cross section area } (mm^2)} \qquad (3)$$

2.4.1.2 Factors Affecting the Test Result

There are many factors affecting the tensile test results:

1. Specimen Preparation and Specimen Size: Molecular orientation has a significant effect on tensile strength values. A load applied parallel to the direction of molecular orientation may yield higher values than the load applied perpendicular to the orientation. The opposite is true for elongation. The process employed to prepare the specimens also has a significant effect. For example, injection molded specimens generally yield higher tensile strength values than compression molded specimens. Machining usually lowers the tensile and elongation values because of small irregularities introduced into the machined specimen. Another important factor

affecting the test results is the location and size of the gate on the molded specimens [18].

2. Rate of Straining: As the strain rate is increased, the tensile strength and modulus increases. However, the elongation is inversely proportional to the strain rate [18].

3. Temperature: The tensile properties of some plastics change rapidly with small changes in temperature. Tensile strength and modulus are decreased while elongation is increased as the temperature increases [18].

2.5 Flow properties

2.5.1 Melt Index Test

The melt index, more appropriately known as melt flow rate (MFR), test measures the rate of extrusion of a thermoplastic material through an orifice of specific length and diameter under prescribed conditions of temperature and load. This test is primarily used as a means of measuring the uniformity of the flow rate of the material. The reported melt index values help to distinguish between the different grades of a polymer. A high-molecular-weight material is more resistant to flow than a low-molecular weight material. However, the data obtained from this test does not necessarily correlate with the processibility of the polymer. This is because plastics materials are seldom manufactured without incorporating additives which affect the processing characteristics of a material, such as stability and flowability. The effect of these additives is not readily observed via the melt index test. The rheological characteristics of polymer melts depend on a number of variables. Since the values of these variables may differ substantially from those in large-scale processes, the test results may not correlate directly with processing behavior [18].

The melt index apparatus is preheated to a specified temperature. The material is loaded into the cylinder from the top and a specified weight is placed on a piston. The material is allowed to flow through the die. The initial extrudate is discarded because it may contain some air bubbles and contaminants. Depending on the material or its flow rate, cuts for the test are taken at different time intervals. The extrudate is weighed and melt index values are calculated in grams per 10 minutes [18].

2.5.1.2 Factors Affecting the Test Results

There are many factors affecting the melt index test results:

1. Preheat Time: If the cylinder is not preheated for a specified length of time, there is usually some nonuniformity in temperature along the walls of the cylinder even though the temperature indicated on the thermometer is close to the set point. This causes the flow rate to vary considerably. There should be zero thermal gradient along the full length of the test chamber.

2. Moisture: Moisture in the material, especially a highly pigmented one, causes bubbles to appear in the extrudate which may not be seen with the naked eye. Frequent weighing of short cuts of the extrudate during the experiments reveals the presence of moisture. The weight of the extrudate is signifiantly influenced by the presence of the moisture bubbles.

3. Packing: The sample resin in the cylinder must be packed properly by pushing the rod with substantial force to allow the air entrapped between the resin pellets to escape. Once the piston is lowered, the cylinder is sealed off, and no air can escape. This causes variation in the test results.

4. Volume of Sample: To achieve the same response curve repeatedly, the volume of the sample in the cylinder must be kept constant. Any change in sample volume causes the heat input from the cylinder to the material to vary significantly [18].

The melt index values obtained from the test can be interpreted in differerent ways. First, a slight variation in the melt index value should not be interpreted as indicating a suspect material. The material supplier should be consulted to determine the expected reproducibility for a particular grade of plastic material. A significantly different melt index value than the control standard may indicate several different things. The material may be of a different grade with a different flow characteristic. It also means that the average molecular weight or the molecular weight distribution of the material is different than the control standard and may have different properties [18].
Melt index is an inverse measure of molecular weight. Since flow characteristics are inversely proportional to the molecular weight, a low-molecular-weight polymer will have a high melt index value and vice versa [18].

2.6 Thermal Conductivity

Thermal conductivity is defined as the rate at which heat is transferred by conduction through a unit cross-sectional area of a material when a temperature gradient exists perpendicular to the area. The coefficient of therrnal conductivity, sometimes called the *K* factor, is expressed as the quantity of heat that passes through a unit cube of the substance in a given unit of time when the difference in temperature of the two faces is 1ºC [18].

The quantity of heat flow depends upon the thermal conductivity of the material and upon the distance the heat must flow. This relationship is expressed as:

$$q \sim k/x \qquad (4)$$

where, q = quantity of heat flow, k = thermal conductivity, x = the distance the heat must flow. Closed-cell structures provide the lowest thermal conductivity owing to the reduced convection of gas in the cells [18].

2.6.1 Thermal Conductivity Measurements by Hot Wire Method

The hot wire method is a standard transient dynamic technique based on the measurement of the temperature rise in a defined distance from a linear heat source (hot wire) embedded in the test material. If the heat source is assumed to have a constant and uniform output along the length of test sample, the thermal conductivity can be derived directly from the resulting change in the temperature over a known time interval [19].

The hot wire probe method utilizes the principle of the transient hot wire method. Here the heating wire as well as the temperature sensor (thermocouple) is encapsulated in a probe that electrically insulates the hot wire and the temperature sensor from the test material [19].

The ideal mathematical model of the method is based on the assumption that the hot wire is an ideal, infinite thin and long line heat source, which is in an infinite surrounding from homogeneous and isotropic material with constant initial temperature. If q is the constant quantity of heat production per unit time and per unit length of the heating wire ($W.m^{-1}$), initiated at the time t=0, the radial heat flow around the wire occurs. Then the temperature rise, $\Delta T(r,t)$, at radial position, r (see Figure 2.7), from the heat source conforms to the simplified formula:

$$\Delta T(r,t) = \frac{q}{4\pi k} \ln \frac{4at}{r^2 C} \qquad (5)$$

where, k is the thermal conductivity ($W.m^{-1}.K^{-1}$), a thermal diffusivity ($m^2.s^{-1}$) ($a=k/\rho c_p$, with ρ is the density ($kg.m^{-3}$) and c_p the heat capacity ($J.kg^{-1}.K^{-1}$) of the test material and C=exp (γ), γ=0,5772157 is the Euler's constant [19].

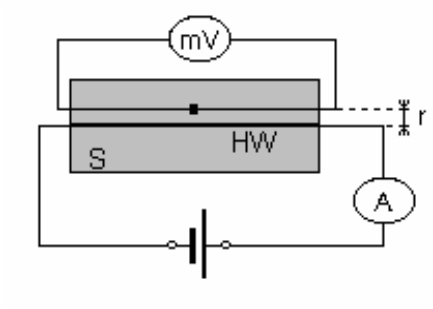

Figure 2.7 Schematic view of the hot wire test sample [19]

The hot wire method can be applied in several experimental modifications. In the standard cross technique the wire cross is embedded in ground grooves between two equally sized specimens. The cross consists of a heating wire and the legs of a thermocouple, which acts as the temperature sensor. The hot spot of the thermocouple is in direct contact with the heating wire. In the resistance technique the heating wire acts also as the temperature sensor. Here the temperature is measured by the change in resistance caused by the heating-up of the hot wire. In the measurement of electrically conducting materials the heating wire and thermocouple wires, or potential leads, are insulated from the sample. This is done either by making of a non-conducting coating on the wires, or to enclose the heater and temperature sensor in a thin sheath or needle probe, which is inserted into the test material, respectively. The second approach is called as the hot-wire-probe method [19].

2.7 Mixing

There are a number of different mixing operations that occur in polymer processing. When the materials to be mixed are solids, the mixing typically involves particulate solids. This type of mixing is referred to as *solid-solid mixing.* When a polymer has to be mixed with a particulate solid and both the polymer(s) and the filler(s) are in powder form, substantial mixing can take place with the use of solid-solid mixing. The remainder of the mixing then is accomplished by melting the polymer/filler mix to

achieve complete wetting of the filler by the polymer. The mixing of the molten polymer with the solid filler is referred to as *solid-liquid mixing* [20].

More typically, the filler is mixed in with the polymer when the polymer is melted. In this case, most of the mixing is solid-liquid mixing. This is the primary mixing action that occurs in plasticating screw extruders. Solid material is fed to plasticating screw extruders and is melted as it is conveyed forward by the rotating screw to the end of the screw [20].

lt is quite common to distinguish two types of mixing, distributive mixing and dispersive mixing. *Dispersive mixing* involves the reduction in size of a cohesive component and is also referred to as *intensive mixing.* An example of dispersive mixing is the mixing of a pigment into a polymer in which the agglomerate size of the pigment has to be reduced below a certain minimum size to obtain good surface quality of the final product. A schematic representation of dispersive mixing is shown in Figure 2.8 [20].

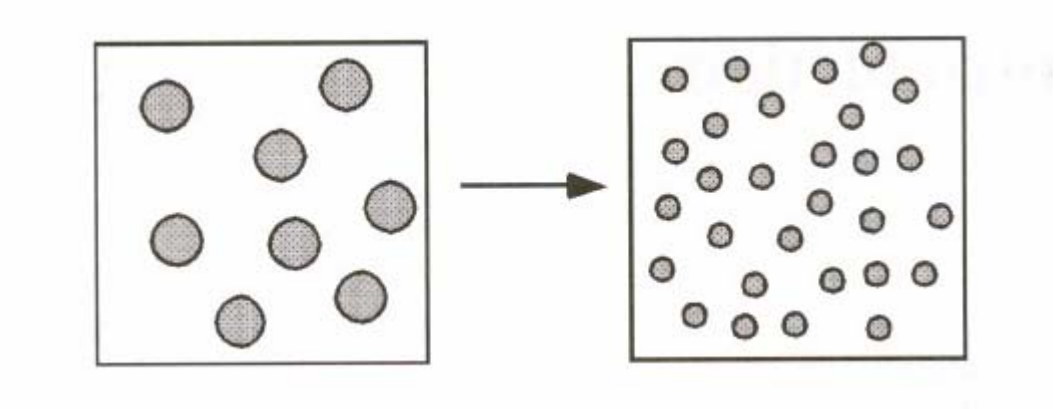

Figure 2.8 Schematic representations of dispersive mixing [20]

Distributive mixing is mixing in the absence of a cohesive resistance and is also referred to as extensive, simple, or nondispersive mixing. An example of distributive mixing is the mixing of two miscible polymer melts, e.g., polystyrene (PS) and

polyphenylene oxide (PPO). Distributive mixing can occur in solids as well as in fluids. When particulate solids are blended without reducing the partide sizes of the solids, this is distributive solid-solid mixing. When a particulate solid is blended into a liquid without reducing the particle size, this is distributive solid-liquid mixing. A schematic representation of distributive mixing is shown in Figure 2.9 [20].

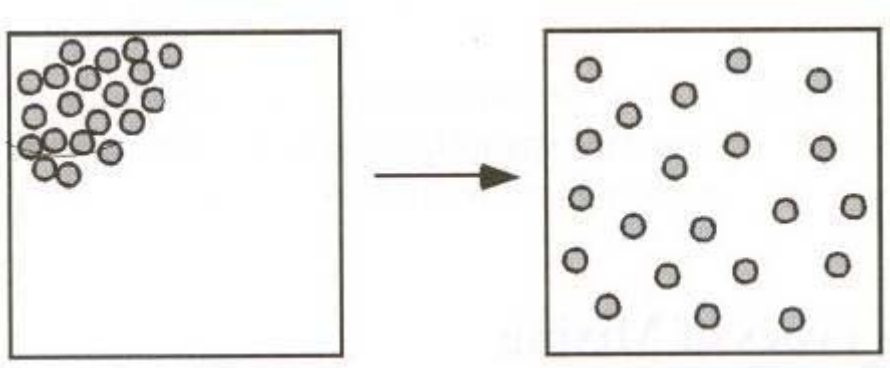

Figure 2.9 Schematic representations of distributive mixing [20]

Mixing can be defined as a process to reduce composition nonuniformity. The basic process involved in mixing is to induce relative motion between the ingredients of the mixture. There are three types of motion that can occur:

1. Diffusion, limited to low molecular weight materials;
2. Turbulent motion, limited to low-viscosity fluid; and
3. Convective motion, prevalent in high-viscosity fluids [20].

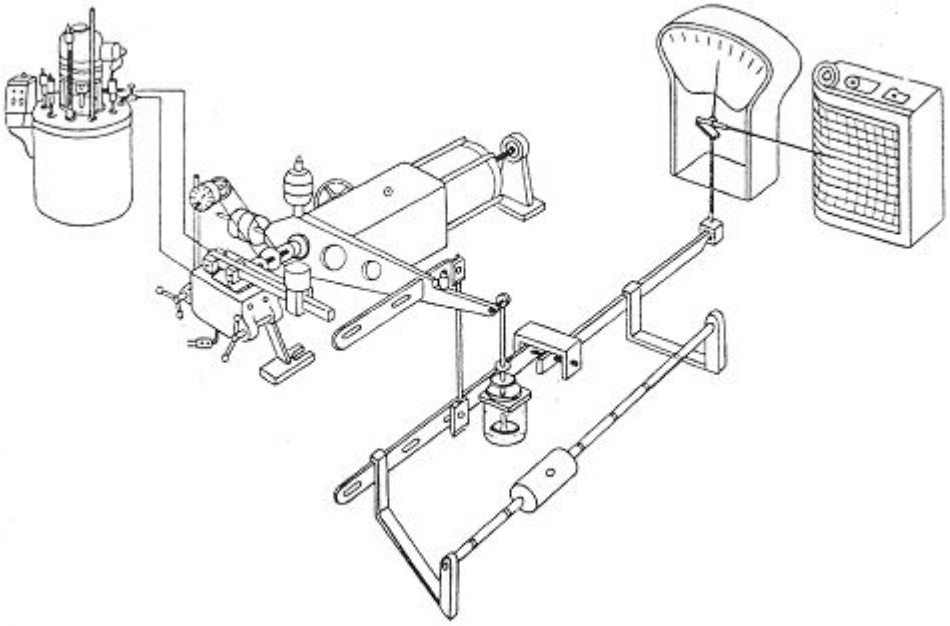

Figure 2.10 Schematic representation of brabender (Courtesy C. W. Brabender Instruments, Inc.) [18]

2.7.1 Internal Mixers

The original internal mixer was developed by Thomas Hancock around 1830. The Hancock masticator used only a single rotor to mix the material. Twin rotor mixers were introduced around 1880 by Werner and Pfleiderer GmbH; the mixing chamber in this machine was not fully enclosed. About forty years later, Banbury introduced an internal mixer equipped with a ram to force the material into the mixing chamber and to provide sealing.The rotors in the Banbury mixer are nonintermeshing and counter-rotating. Intermeshing counter-rotating internal mixers were introduced by Cooke of Francis Shaw and Company and by Lasch and Stromer of Werner and Pfleiderer. Most internal mixers use counter-rotating rotors, but Brennan from Teledyne-Readco developed a co-rotating internal mixer. Figure 2.10 illustrates a commercially available torque rheometer [20].

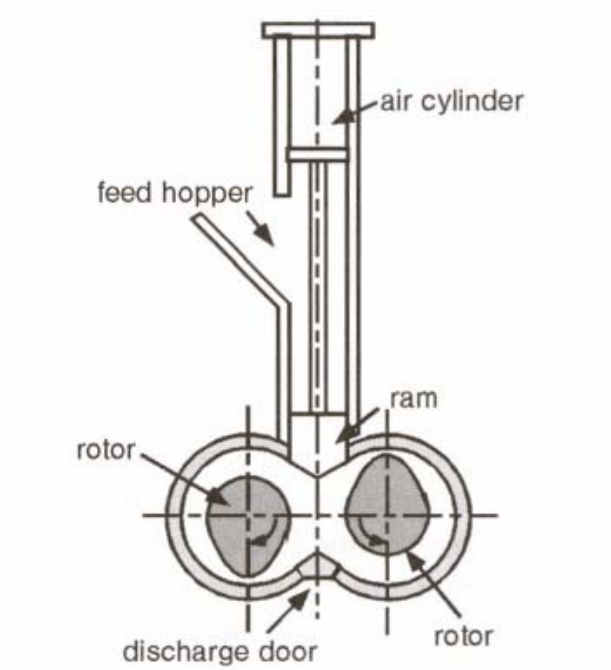

Figure 2.11 Schematic representation of a batch internal mixer [20]

The main components of a batch internal mixer are the rotors, the mixer housing, the ram, the ramair cylinder, the feed hopper, and the door for discharge (Figure 2.11). The advantages of the batch internal mixer are:

1. It accepts feed stock in various forms,
2. It has intensive mixing action,
3. It has a well-defined residence time,
4. Quick material changes can made, and
5. A wide range of mixing procedures can be used [20].

The mixing action of the internal rnixer is concentrated in the narrow gaps between the rotor and the housing. In these regions, high rates of shear and elongation occur, resulting in intensive mixing action. Because the mixer is usually equipped with high horse power drives, the mixer can handle high-viscosity materials quite well. Some disadvantages of the batch internal mixer are:

1. It is not a self-wiping mixing device,
2. Batch-to-batch variations can affect product quality,
3. It is difficult to achieve fine process control, and
4. It cannot handle high-temperature engineering plastics [20].

2.7.1.1 Order of Addition of Ingredients

The sequence of the addition of the ingredients is key to good mixing in internal mixers. Generally, the objective is to arrange the sequence to maintain adequate stiffness in the mixture until the most difficult step in the dispersion is achieved. Anormal sequence of mixing of a filled polymer is as follows:

Step 1. Load polymer and one-half of the filler and mix until the material softens.
Step 2. Add remaining filler and mix until fully incorporated.
Step 3. Add plasticizers and/or softeners and complete mixing [20].

In some cases, a batch may soften too quickly before a good dispersion is obtained. In this case, an alternate technique may be used, referred to as "upside down mixing". In this technique, all ingredients are added at once, maximum ram pressure is applied, and maximum rotor speed is used. The main process variables in the batch mixing process are batch weight (fill factor), material feed temperature, mixer temperature, rotor speed, ram pressure, and sequence and timing of the feeding of the ingredients [20].

2.7.1.2 Degree of Fill and Rotor Speed

The mixing efficiency in the batch internal mixer is strongly influenced by both the degree of fill of the mixer and the rotor speed. Both these variables were studied by Ries, and the results are represented in Figure 2.12. The quality of the mix is plotted along the vertical axis, with the degree of fill along the horizontal axis. The mix quality

of 6 is poor and 0 is the best; these rankings are based on the dispersion of the carbon black in the mixture [20].

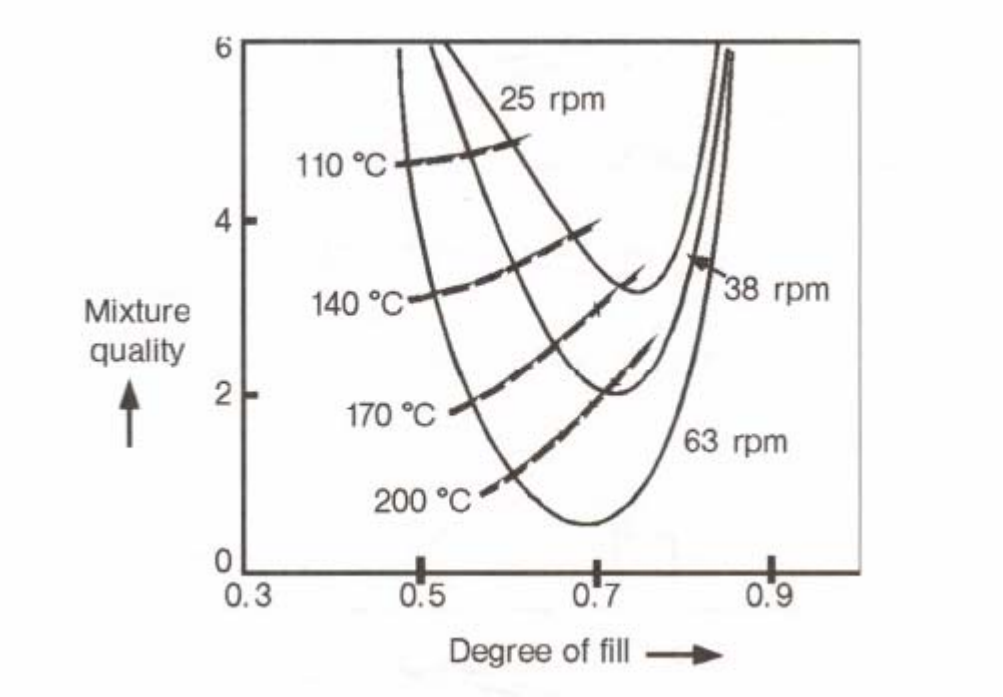

Figure 2.12 Mixture quality vs. degree of fill at three rotor speeds [20]

Figure 2.12 shows that the optimum degree of fill is in the range of 70 to 80%. At low rotor speed, the optimum degree of fill is ~80%, but the best mix quality achieved is marginal, around three. At high rotor speed, the optimum degree of fill is ~70%; however, at this level of fill the quality of the mix is much better than at lower rotor speed. It is clear that the wrong degree of fill can be quite detrimental to the mix quality [20].

The discharge melt temperature is also indicated in Figure 2.12. As the rotor speed and the dispersion quality increases, the stock temperature increases as well. In some cases, the discharge melt temperature will limit the rotor speed that can be used. This can be the case when the material has limited thermal stability at elevated temperatures or when the material may cross-link at high temperatures. If high rotor

speed is desired, the geometry of the rotor can be adapted to run at higher than normal speed [20].

2.8 Previous Studies

Fritschy and Papirer [21] studied interactions between bitumen and silicas by using solution adsorption techniques. They demonstrated that the reactive part of the bitumen is the asphaltene which forms, by chemisorption on the silanol groups of the silica, a monolayer having a thickness which compares fairly well with the published dimensions of the asphaltene molecules. They concluded that adsorption of the asphaltenes onto other pigments shows the specificity of the interaction.

Craus et al. [22] investigated factors affecting selective sorption in the bitumen-filler interface and the difference in the capacity of various fillers for selective sorption of the chemical groups combining the bitumen. They evaluated selective sorption quantitativly by using a chromatographic method and investigated that, hydrated lime and limestone were the most effective, basalt was intermediate, while sandstone and mainly glass beads showed almost no capacity for selective sorption. They stated that evaluation of selective sorption capacity of the filler is of great importance because of surface activity properties of filler constitutes influence the mechanical properties of the bitumen-filler system and the behaviour of the mixture. For this reason, they studied the behaviour of sand asphalt mixtures with different types of filler. They concluded that results were in agreement with the behaviour of the different fillers under selective sorption.

Dubey et al. [23] studied effect of adsorbed asphaltenes on rock wettability and asphaltene adsorption/desorption on clay minerals, silica, and carbonates. They examined the effect of solvent variation for asphaltene adsorption on the clay mineral kaolin. They evaluated the ability of solvents to remove asphaltene from kaolin and formation core material by screening pyrolysis-flame-ionization-detection (P-FID) test.

Ulf Isacsson et al. [24] studied the effect of filler on low temperature physical hardening of bitumen by using a Bending Beam Rheometer. They used hydrated lime and calcium carbonate as fillers and evaluted the effect of the fillers on the isothermal low temperature hardening. They investigated the viscoelastic nature of the bitumens and bitumen-filler mixtures. As a result of this study, they concluded that the dissipation energy ratio is not necessarily related to the stiffness of the binder.

A. Perez-Lepe et al. [10] studied the influence of the processing conditions on the rheological behaviour of polymer-modified bitumen. They prepared polymer modified bitumen composites by using 50/70 and 150/200 penetration grades bitumens and number of polymers like HDPE, LDPE, SBS and EPDM. They studiied the influences that processing variables exert on the rheological properties of polymer-modified bitumens. It was obtained that a rotor–stator mixer device enhances the rheological properties of binders prepared with high-density polyethylene, low-density polyethylene, ethylene–propylene–diene monomer, and their blends, as compared to a stirred tank device.

Ven and Jenkins [25] were reported some rheological properties of the bitumen and bitumen/filler system as sub-systems of the mix. Results of their work were presented for the rheological characterisation of bitumen-rubber and SBS modified bitumen compared to standard bitumen. They investigated the effect of filler addition also. The filler/bitumen ratio in all cases was 1:1 by mass in their study. Dynamic Shear Rheometer was used for three types of testing: strain sweeps; frequency sweeps and high temperature viscosity testing. They concluded viscosity properties at mixing and compaction temperature of SBS modified binders differs from normal penetration grade bitumen and polymer addition improves binder response to loading at service temperatures.

K. Baginska and I. Gawel [26] investigated the effect of origin and technology on the chemical composition and colloidal stability of bitumens in 2004. They analyzed 50 and 70 penetration grades of bitumen for generic composition, macrostructure and

colloidal stability. The bitumens they studied exhibited a satisfactory colloidal stability. They concluded that the slightly higher colloidal stability parameter of bitumens from naphthenic crude oil is likely to be due to a smaller aggregation of asphaltene micelles and greater resins to asphaltenes ratio in these bitumens.

Little et al. [27] evaluated hydrated lime as a filler in bitumen and compared to similarly sized filler comprised of calcium carbonate, limestone. They made several rheological tests. According to this study, it was seen that hydrated lime as a filler significantly impacts the rate and level of microcrack-induced damage, microdamage healing, and plastic and viscoelastic flow in both mastics and mixtures across a wide range of temperatures. They also concluded that, the impact of hydrated lime as a filler is dependent on its interaction with a specific bitumen.

M. Karaşahin and S. Terzi [28] prepared samples having limestone dust and marble dust filler and determined optimum binder content. They also determined optimum filler content by considering the filler/bitumen ratio and filler ratio. They determined that test results of the samples containing the marble dust and limestone dust have almost similar plastic deformations. They concluded that asphalt mixtures containing marble dust can be used directly in the mix without any process.

CHAPTER 3

EXPERIMENTAL

3.1 Materials

3.1.1 Bitumen

In this study, bitumen which was purchased from TÜPRAŞ A.Ş. was used as basic material for all samples. It played an important role acting as a binder. Two different bitumen grades were used; 20/30 penetration bitumen and 50/70 penetration bitumen. 20/30 penetration grade is stiffer and more viscous, 50/70 penetration grade is softer and more sensitive to temperature. Table 3.1 and Table 3.2 show the physical properties of bitumen that used in this work.

Table 3.1 Properties of 50/70 penetration grade bitumen used in the study.

Property	ASTM	Unit	Value
Penetration at 25 ^{0}C, 100 g, 5 sec	D 5	x 0.1 mm	50/70
Softening Point (ring and ball method)	D 36	^{0}C	46-54
Solubility (in dichloroethane)	D 2042	Wt %	99

Table 3.2 Properties of 20/30 penetration grade bitumen used in the study.

Property	ASTM	Unit	Value
Penetration at 25 ^{0}C, 100 g, 5 sec	D 5	x 0.1 mm	20/30
Softening Point (ring and ball method)	D 36	^{0}C	57-67
Solubility (in dichloroethane)	D 2042	wt %	98
Ductility at 25 ^{0}C, 5 cm/min	D113	cm	15

3.1.2 Fillers

In this work, several fillers were used with different concentrations. $CaCO_3$ were used as main filler for all of the samples. CaO, baryte, mica, kieselguhr are the fillers which were used separately with different ratios. In some cases, kieselguhr was exposed surface silanation process before using.

3.1.2.1 Calcium Carbonate ($CaCO_3$)

The trade name of $CaCO_3$ used in this work is OMYACARB 3 EXTRA- GZ which was supplied from Omya Minning, İstanbul, Turkey. Tables 3.3 and 3.4 show the chemical composition and physical properties of $CaCO_3$ used in this work, respectively.

Table 3.3 Chemical composition of $CaCO_3$

Material	Composition (%)
$CaCO_3$	98.5
$MgCO_3$	1.5
Fe_2O_3	0.05

Table 3.4 Physical properties of $CaCO_3$

Property	Value
Average particle size	5 µm
pH value	9.5
Density	2.7 g/cm^3

3.1.2.2 Calcium Oxide (CaO)

The trade name of CaO used in this work is Super 40 Weißfeinkalk CL 90 which was supplied by Märker Kalk GmbH, Hamburg, Germany. The chemical composition of CaO is shown in Table 3.5.

Table 3.5 Chemical composition of CaO

Material	Composition (%)
CaO	94.0
MgO	0.4
CO_2	2.0
SiO_2	0.8
Fe_2O_3	0.2
Al_2O_3	0.3
SO_3	0.2

3.1.2.3 Mica

Mica was the another filler used in this study which trade name is MICA 900 was purchased from Aspanger Bergbau und Mineralwerke GmBH. Chemical composition of mica is represented in Table 3.6.

Table 3.6 Chemical composition of mica

Material	Composition
SiO_2	45.6
Al_2O_3	32.4
K_2O	10.4
CaO	<0.08
Fe_2O_3	5.00
MgO	0.70
TiO_2	0.68
P_2O_5	<0.01
MnO	0.01

3.1.2.4 Baryte (Barium Sulphate)

BB 20-40/94 is the trade name of baryte used which was obtained from Baser Mining Ind. & Com. Inc., Antalya, Turkey. Chemical composition of baryte is given in Table 3.7. Baryte has nano scale pores which can be deduced from Table 3.8. The oil absorption capacity of baryte is given as 14-16 ml/100 g baryte. This value corresponds to about 30 % porosity for baryte. The pore size of baryte is much smaller than the pores in kieselguhr.

Table 3.7 Chemical composition of baryte

Material	Composition (%)
$BaSO_4$	95.30
SiO_2	0.08
Fe_2O_3	0.05
CaO	1.04
Al_2O_3	0.01

Table 3.8 Particle Size Distribution of Baryte and Technical Properties of Baryte

Particle Size Distribution	
(Malvern Mastersizer Microplus Ver 2.18)	
Mean Particle Size (d_{50})	4.0 max
Top cut (d_{98})	22.0 max
2 microns passing	% 40.0 min
Technical Properties	
Specific Gravity (ISO 787/10)	g/ml 4.38
Hardness (Moh's)	3.25
Bulk Density (ISO 787/11)	g/ml 1.70-1.85
pH (ISO 787/9)	8.50
Moisture (ISO 787/2)	0.10%
Oil Absorption (ISO 787/5)	ml/100g 14-16
Refractive Index	1.64

3.1.2.5 Kieselguhr (diatomaceous earth)

Kieselguhr was purchased from Ceca, Paris, France. Trade name of the kieselguhr used in this study is Clarcel FD and it is obtained by flux calcinations and particle size selection of a diatomaceous earth. It is composed of more than 85% of silica. Tables 3.9, 3.10, 3.11 represent chemical composition, physical properties and particle size distribution of Clarcel FD.

Table 3.9 Chemical Composition of Clarcel FD

Material	**Composition (%)**
SiO_2	91.5
Al_2O_3	2.9
Fe_2O_3	1.5
TiO_2	0.075
CaO	1.1
MgO	0.2
K_2O	0.5
Na_2O	2.0

Table 3.10 Physical Properties of Clarcel FD

Method	Property	Unit	Value
140 1308	Oil absorption	$cm^3/100g$	140
140 1311	Moisture	%	0.5
140 1312	Loss on ignition	%	0.5
140 1310	Whiteness	-	≥ 86
140 1303	Retained at 50µm	% in weight	≤ 0.5

Table 3.11 Particle Size Distribution of Clarcel FD

Particle size distribution	Volume percent
1 µ	95.5
> 5 µ	65.4
> 10 µ	34.4
> 20 µ	7.4
> 35 µ	2.0
> 50 µ	0.8
> 75 µ	0.3
> 100 µ	0.2
> 200 µ	0
> 350 µ	0
> 500 µ	0

3.1.3 Polymers

Styrene Butadiene Styrene Block Copolymer (SBS), Ethylene Vinyl Acetate (EVA) and Styrene Butyl Rubber (SBR) were used as polymers in this study.

3.1.3.1 EVA

Alcudia® PA-461 is trade name of EVA used in this study which was supplied by Alcudia. Typical properties of Alcudia® PA-461 are given in Table 3.12.

Table 3.12 Properties of Alcudia® PA-461

Property	Unit	Value
Melting point	^{0}C	59 – 64
Density @ 23°C	kg/m^2	956
Vinyl Acetate content	%	33
Melt Flow Rate (190°C, 2.16kg)	g/10 min	45

3.1.3.2 SBS

Trade name of SBS used in this work is Elastron D® which was supplied by Elastron Kimya San. ve Tic. A.Ş., Turkey. Elastron D® is the brand name of a family compounds based on styrenic block copolymer SBS (styrene-butylene-styrene) and polyolefins (PP or PS), which shows some of the rubber properties and has the advantage of easy processing. Physical and mechanical properties of Elastron D® are shown in Table 3.13.

Table 3.13 Physical and Mechanical Properties of Elastron D®

Method	Property	Unit	Value
ASTM D 2240	Hardness	(Shore A)	70 ± 2
ASTM D 792	Specific Gravity	g/cm^3	1.03 ± 0.02
ASTM D 412	Tensile Strength at Break	kgf/cm^2	65 ± 7
ASTM D 412	Elongation at Break	%	750 ± 100
ASTM D 624	Tear Resistance	N/mm	50

3.1.3.3 SBR

SBR was purchased from Lukoil Bulgaria Ltd., Sofia, Bulgaria. Trade name of SBR is Bulex® L-108. Table 3.14 shows the properties of Bulex® L-108 used in this work.

Table 3.14 Properties of SBR Latex

Property	Unit	Value
Total solids, not less than	% wt	65
Surface tension	mN/m	33 ± 2
Brookfield viscosity, not higher than	$mN.s/m^2$	1000
pH		9.5 - 11
Residual styrene, not more than	% wt	0.04
Bound styrene	% wt	36-39

3.1.4 Silicone Oil

Silicone oil was purchased from Aklar Kimya which has viscosity of 1000 mPa.s. Figure 3.1 represents the general molecular formula of silicone oil. 2 % acetone solution of silicon oil was used for surface silanation process.

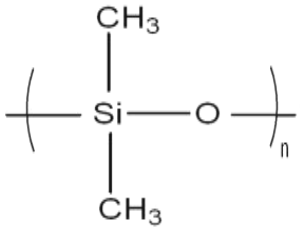

Figure 3.1 General molecular formula of silicone oil

3.2 Experimental

3.2.1 Filler type and ratio

In this study, the five different types of fillers were used at various volume fractions. $CaCO_3$ was used as the basic filler material for all of the samples. Main purpose of using $CaCO_3$ with bitumen was to produce a stiffer and harder material. Different types of polymers were also used in order to increase the mechanical properties of some samples.

CaO was used all of the samples at 2 vol. % for its ability to hold moisture. Baryte, mica, kieselguhr, and silaned kieselguhr were used at different concentrations. Table 3.15 represents the volume percent compositions of composites investigated in this study.

Table 3.15 Compositions of bituminous composites (vol. %)

Sample No	Bitumen (20/30)	Bitumen (50/70)	$CaCO_3$	CaO	Baryte	Mica	Silaned Kieselguhr	Kieselguhr	EVA	SBR	SBS	Tensile Strength	Percentage Strain
1	18.0	22.0	50.0	2.0	-	2.0	-	-	-	-	6.0	3.6	4.0
2	18.0	22.0	53.0	-	-	2.0	-	-	5.0	-	-	4.8	4.1
3	19.0	22.0	54.0	2.0	-	-	-	-	2.0	0.2	0.4	3.5	8.0
4	19.0	22.0	52.0	2.0	-	2.0	-	-	2.0	0.3	0.4	4.2	5.6
5	20.0	23.0	45.0	2.0	7.0	-	-	-	2.0	0.3	0.5	4.3	7.1
6	20.0	23.0	40.0	2.0	10.0	2.0	-	-	-	-	3.0	1.6	13.8
7	21.0	25.0	32.0	2.0	15.0	2.0	-	-	2.0	0.4	0.5	3.7	6.8
8	21.0	25.0	34.0	2.0	15.0	-	-	-	2.0	0.4	0.5	3.3	9.6
9	22.0	27.0	15.0	2.0	30.0	-	-	-	3.0	0.4	0.5	2.5	9.4
10	24.0	30.0	-	2.0	40.0	-	-	-	3.0	0.4	0.5	2.2	10.1
11	20.0	24.0	44.0	2.0	-	2.0	-	5.0	-	-	3.0	2.2	7.7
12	-	50.0	40.0	-	-	-	-	10.0	-	-	-	1.5	19.3
13	22.0	26.0	33.0	2.0	-	-	-	15.0	2.0	-	-	5.1	6.0
14	-	50.0	30.0	-	-	-	-	20.0	-	-	-	1.1	16.2
15	-	50.0	40.0	-	-	-	10.0	-	-	-	-	1.3	3.5
16	17.0	21.0	45.0	2.0	-	2.0	10.0	-	-	-	3.0	2.1	8.2
17	22.0	27.0	34.0	2.0	-	-	15.0	-	-	-	-	1.8	8.7
18	-	50.0	30.0	-	-	-	20.0	-	-	-	-	0.5	30.2
19	16.0	19.0	38.0	2.0	-	2.0	20.0	-	-	-	3.0	2.3	9.2
20	19.0	22.0	31.0	2.0	6.0	-	20.0	-	-	-	-	2.5	15.1
21	16.0	19.0	36.0	2.0	-	2.0	25.0	-	-	-	-	1.9	8.3
22	16.0	19.0	35.0	2.0	-	-	25.0	-	-	-	3.0	2.1	49.4
23	16.0	19.0	35.0	2.0	-	-	25.0	-	3.0	-	-	3.3	4.0
24	-	50.0	20.0	-	-	-	30.0	-	-	-	-	0.4	28.0

3.2.2 Silane Treatment of Kieselguhr

Kieselguhr was silaned by using 2 % silicon oil containing acetone mixture. The mixture and Kieselguhr were stirred about 2 hours. After that, acetone was allowed to evaporate in open air. Silaned kieselguhr was dried and a free flowing powder is obtained. The aim of silanation process is to make kiesel guhr surface and pores non-wettable and create voids containing kieselguhr powder in composite structure.

3.3 Sample Preparation

3.3.1 Mixing

A counter-rotating internal mixer was used in order to obtain several bituminous composites. The model of the internal mixer is Brabender Plasti-Corder Torque Rheometer, PLV-151. Figure 3.2 represents internal mixer used for this study. Materials were added in the order of bitumen, filler, polymer and mixed 15 min with constant screw speed of 60 rpm. Process temperature that was applied for each sample was 180 ^{o}C except for silaned kieselguhr contained materials which was 120 ^{o}C not to expose silane to high temperatures.

Figure 3.2 Brebender internal mixer used in this work

3.3.2 Compression Molding

The specimens for mechanical and thermal characterization were prepared by compression molding using a laboratory scale hot-press machine (Rucker PHI). Figure 3.3 is the schematic view of hot-press machine used. During molding; Press temperature (100°C) and compression pressure (10 bars) were identical for the preparation of each sample. Compression molding was applied for each sample at least 5 times to avoid microbubbles formation inside materials. Samples were handled as casts with 3 mm thickness for tensile test measurements and 1 cm thickness for thermal test measurements which was identical for all materials. Samples were cooled spontaneously and waited one day at room temperature for allowing orientations inside the materials. Then, casts of samples with 3 mm thickness were shaped by using a dog-bone mold with the same hot-press machine at room temperature for tensile test measurements. At least 5 dog-bone shaped speciments were prepared. Casts of samples with 1 cm thickness were shaped with a mold which had dimensions of 7 cm, 15 cm and thickness of 1 cm for thermal test measurements.

Figure 3.3 Schematic representation of hot-press machine used in this work

3.4 Characterization

3.4.1 Morphological Analysis

3.4.1.1 Scanning Electron Microscopy (SEM) Analysis:

Tensile fractured surfaces were examined by a JEOL JSM-6400 Scanning Electron Microscope. Before SEM photographs were taken, the fractured surfaces were coated with a thin layer of gold in order to obtain a conductive surface. The SEM photographs were taken at x250 and x2500 magnifications.

3.4.2 Mechanical Analysis

Tensile tests were performed to observe the mechanical properties of the materials. At least five samples were used for each composition set and the standard deviations were calculated in addition to average values of Tensile strength, Strain at break and Young's modulus.

3.4.2.1 Tensile Test

Tensile tests were performed following the procedure specified in ASTM 638-M 91a (Standard Test Method for Tensile Properties of Plastics) by using a Lloyd LR 5K computer controlled tensile test machine. Figure 3.4 shows the typical example of tensile test of a sample.

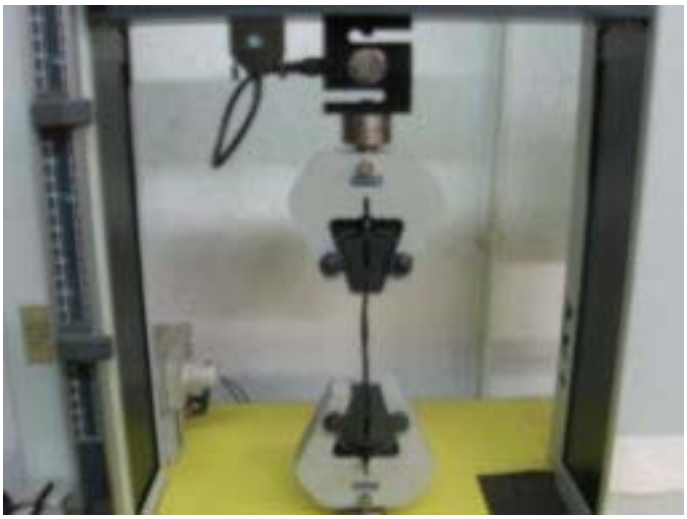

Figure 3.4 The view of a specimen on tensile test machine.

The shape and dimensions of the specimens are illustrated in Figure 3.5 and Table 3.16 respectively. Tensile strength, Young's modulus, and strain at break values were reported for each specimen. The distance between the grips (D), width (W), and thickness (T) were 93, 12.3 and 3 mm respectively.

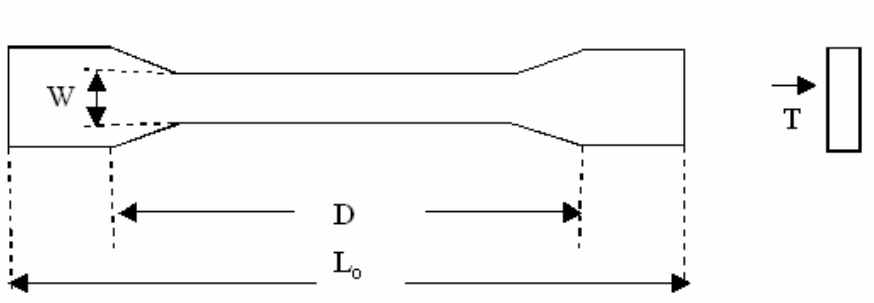

Figure 3.5 Tensile test specimen [29]

Table 3.16 Tensile test specimen dimensions

Symbol	Specimen Dimensions (mm)
W, Width of narrow section	12.3
D, Distance between grips	93.0
L_0, Total length of specimen	140.0
T, Thickness of specimen	3.0

3.4.3 Thermal Analysis

3.4.3.1 Thermal Conductivity Test

Thermal conductivity tests were performed according to hot wire test method (ASTM C 177, TS 4360-1, EN 993-14) at Turkish Standards Institute (TSE) laboratories. Figure 3.6 shows Thermal Conductivity Test Equipment that was used for this study. Results were recorded as W/mK.

Figure 3.6 Thermal Conductivity Test Equipment [30]

3.4.4 Flow Characteristics

3.4.4.1 Melt Flow Index (MFI) Test

Melt flow index (MFI) was performed in order to investigate the flow behavior of the samples, which is inversely related to melt viscosity. The MFI values gave demonstrate effect of fillers on rheological characteristics of the materials prepared in this work.

Melt flow property measurements were studied by using Coesfield Material Test, Meltfixer LT. The measuerements were done at two temperatures of 130 ^{o}C and 180 ^{o}C. Materials were allowed to melt in the instrument for 5 minutes. Then standard weight placed on the piston of the instrument to compress the sample. After that, the weight of the flow sample was recorded as grams/10 min (g/10min). The test was carried out under two specified loads of 2.16 kg and 5 kg. The melt flow index machine used in this study is shown in Figure 3.7.

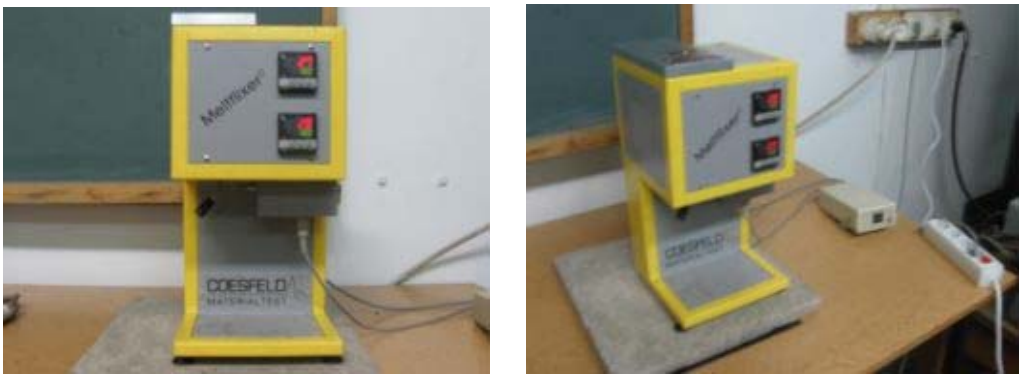

Figure 3.7 Photographs of Coesfeld Melt Flow Indexer

3.4.5 Density Measurements

3.4.5.1 Density Measurements of Samples

Densities of prepared samples were measured by using electronic densitometer MD-300S, Alfa Mirage Co., Ltd.

3.4.5.2 Density Measurements of Fillers

Specific gravities of filler powders were measured by using a dry and clean picnometer which has 25 ml capacity at 25 ^{o}C.

3.4.5.3 Tapped Density Measurements

Tapped densities of kieselguhr and silaned kieselguhr were measured by tapping them in a cylindirical vessel with specified volume until material fill vessel completely.

3.4.6. Particle and Surface Characterizations

3.4.6.1 Mercury Porosimeter

Particle Size distribution and porosity of fillers were determined with Mercury porosimeter, Poremaster 60. Measurements were carried out on samples in forms of pellets of fine powders of fillers.

CHAPTER IV

RESULTS AND DISCUSSION

4.1 Morphological Analysis

4.1.1 Scanning Electron Microscopy (SEM)

Scanning electron microscopy analysis was performed in order to observe the effect of filler type and concentration on the morphology of the prepared bituminous materials. Tests were performed on tensile test fractured surfaces of the prepared materials. The SEM micrographs are presented at x250, x1500, x2000 and x2500 magnifications. Compositions of samples in SEM analysis are represented in Table 4.1.

Table 4.1 Volume percentages of samples in SEM analysis

Sample No	Bitumen (20/30)	Bitumen (50/70)	$CaCO_3$	CaO	Baryte	Mica	Silaned K.G.	Kieselguhr	EVA	SBR	SBS
1	18.0	22.0	50.0	2.0	-	2.0	-	-	-	-	6.0
2	18.0	22.0	53.0	-	-	2.0	-	-	5.0	-	-
4	19.0	22.0	52.0	2.0	-	2.0	-	-	2.0	0.3	0.4
5	20.0	23.0	45.0	2.0	7.0	-	-	-	2.0	0.3	0.5
10	24.0	30.0	-	2.0	40.0	-	-	-	3.0	0.4	0.5
12	-	50.0	40.0	-	-	-	-	10.0	-	-	-
14	-	50.0	30.0	-	-	-	-	20.0	-	-	-
15	-	50.0	40.0	-	-	-	10.0	-	-	-	-
18	-	50.0	30.0	-	-	-	20.0	-	-	-	-

Figures 4.1 and 4.2 show the fracture surfaces of samples containing 7 and 40 volume percents of baryte, respectively. It is clearly observed that, baryte particles were well-dispersed in material. Sample containing 40 vol. % of baryte does not contain calcium carbonate, interactions between bitumen and baryte molecules when compared with those of calcium carbonate molecules are weaker as seen from Figure 4.2.

Figure 4.3 is the micrograph of sample that contains mica at 2 vol. %. Because of mica has plate-like structure, deep crack lines are observed.

Fracture surfaces of materials containing kieselguhr at 10 and 20 vol. % are presented in Figures 4.4 and 4.5 respectively. The volume percentages are calculated from mass percentages taking 77 % porosity for kieselguhr found by density measurements. The bitumen phase can be seen in Figure 4.4, but not in Figure 4.5, almost all of the bitumen phase penetrated into kieselguhr. As a result of this situation, not enough bitumen remains to bind kieselguhr and calcium carbonate particles and wide voids form, so material crumbles easily with the application of small amount of force. The effect of 50/70 penetration bitumen is another factor for this situation. Because of 50/70 penetration bitumen is less viscous than 20/30 penetration, it more easily impregnates kieselguhr. The effect of silane treatment of kieselguhr on morphological aspect of prepared material is observed in Figures 4.6 and 4.7. In comparison to Figure 4.4 and 4.5, formation of bitumen phase observed around kieselguhr particles which means that impregnation of bitumen molecules into kieselguhr powder is rendered negligible by surface modification with silane. It is seen from Figure 4.7 that, the silane treatment results in partial impregnation of bitumen. In summary, silane treatment prevents the impregnation of bitumen into porous structure of kieselguhr.

Figures 4.8 and 4.9 represent SEM micrographs of materials containing 5 % EVA and 6 % SBS, respectively. It is observed in both of these figures that, polymers, because they were used at low concentrations, are dispersed homogeneously in bitumen phase and they do not form a polymer phase in material. In general, at a low polymer

content, the small polymer spheres swollen by bitumen compatible fractions (e.g. aromatic oils), and, are spread homogeneously in a continuous bitumen phase [31].

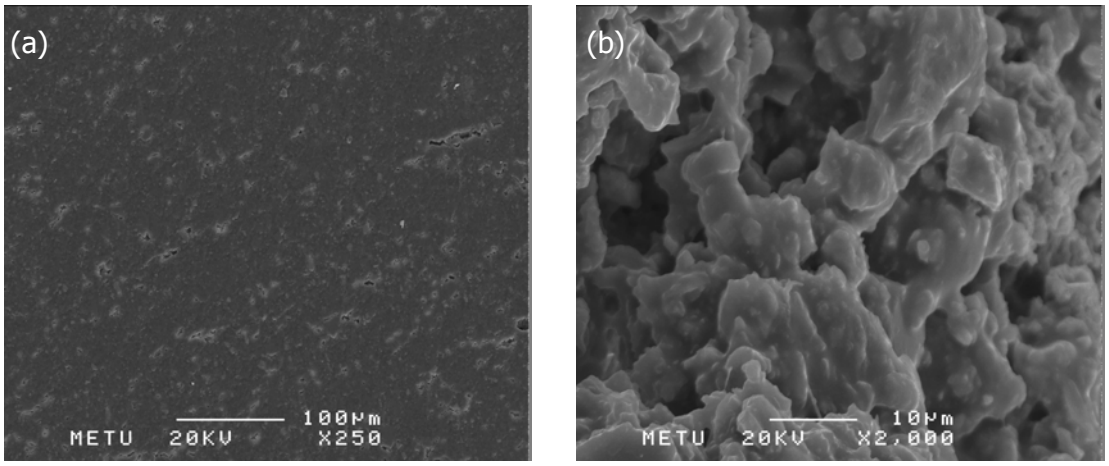

Figure 4.1 SEM micrographs of the material containing 7 vol. % Baryte at (a) x250, (b) x2000 magnifications.

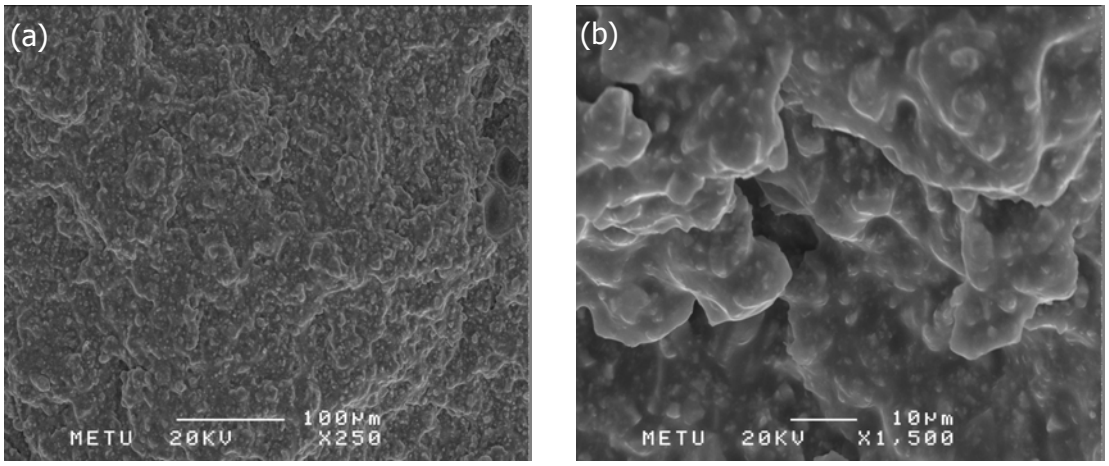

Figure 4.2 SEM micrographs of the material containing 40 vol. % Baryte at (a) x250, (b) x1500 magnifications.

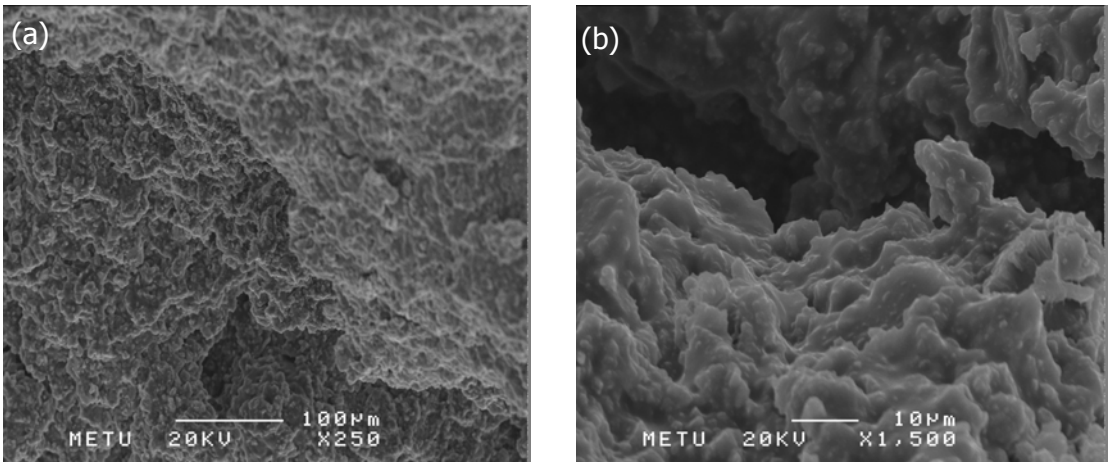

Figure 4.3 SEM micrographs of the material containing 2 vol. % Mica at (a) x250, (b) x1500 magnifications.

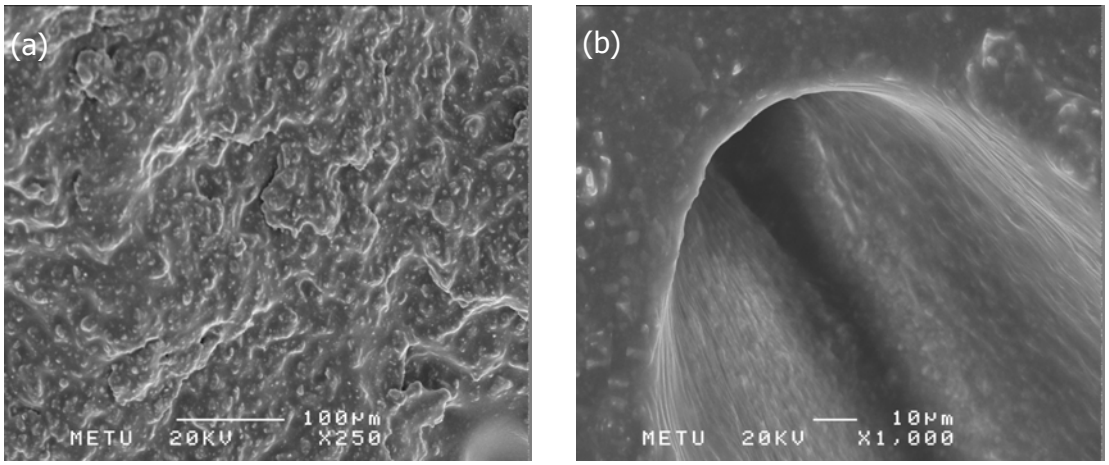

Figure 4.4 SEM micrographs of the material containing 10 vol. % Kieselguhr at (a) x250, (b) x1000 magnifications.

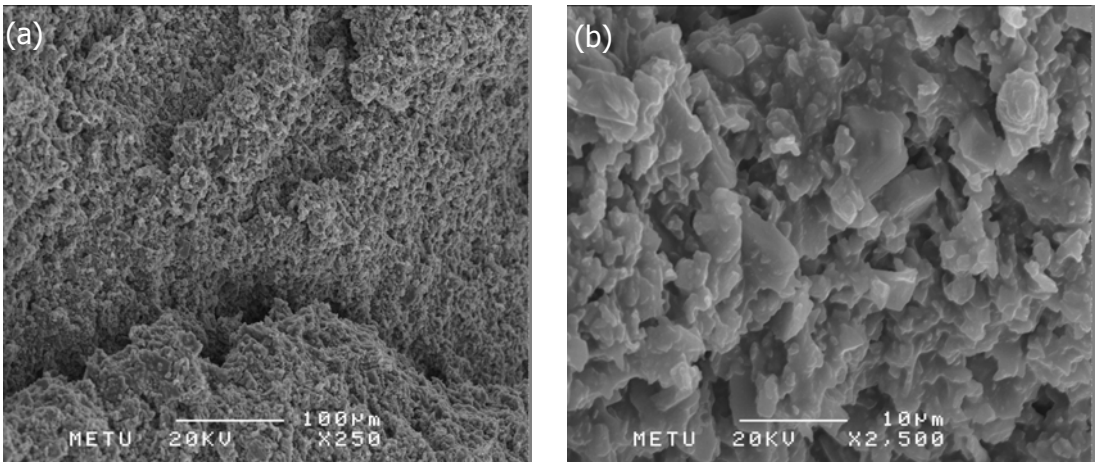

Figure 4.5 SEM micrographs of the material containing 20 vol. % Kieselguhr at (a) x250, (b) x2500 magnification

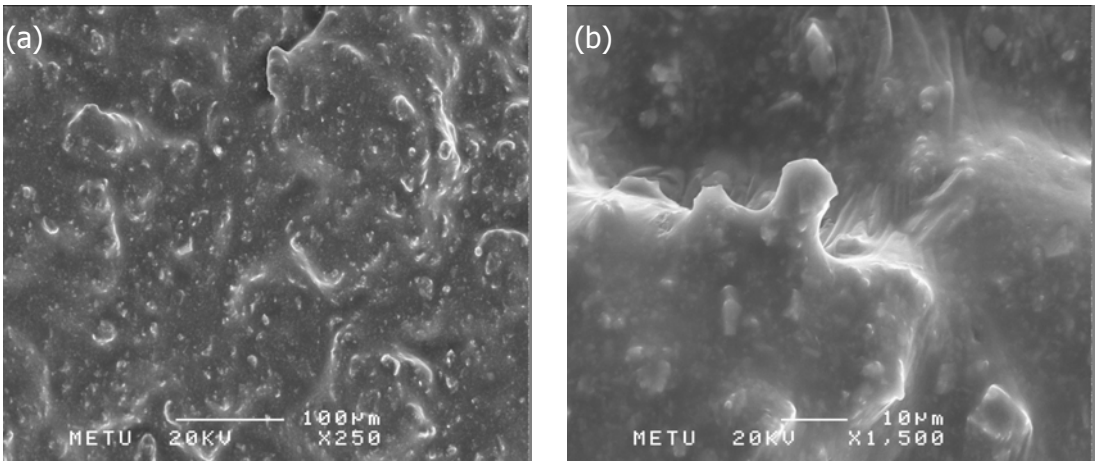

Figure 4.6 SEM micrographs of the material containing 10 vol. % Silaned Kieselguhr at (a) x250, (b) x1500 magnifications

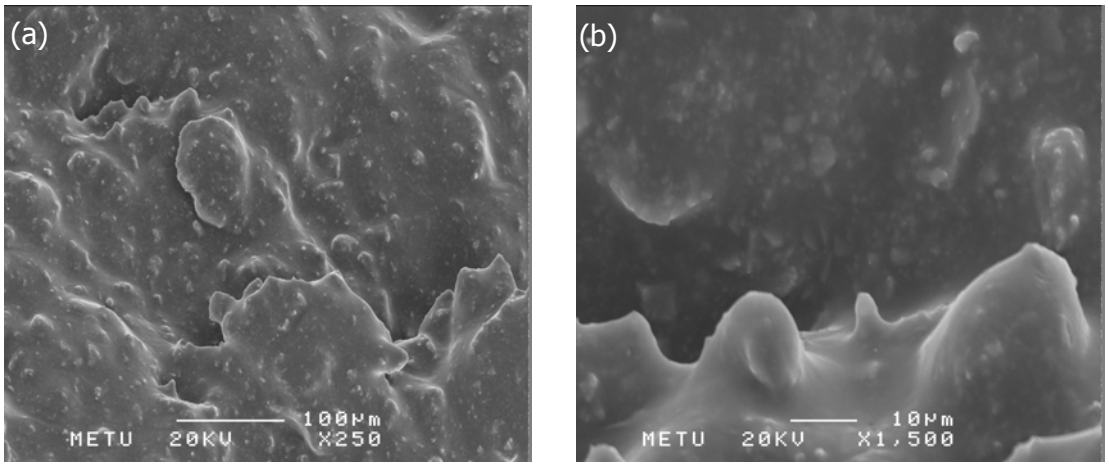

Figure 4.7 SEM micrographs of the material containing 20 vol. % Silaned Kieselguhr at (a) x250, (b) x1500 magnifications

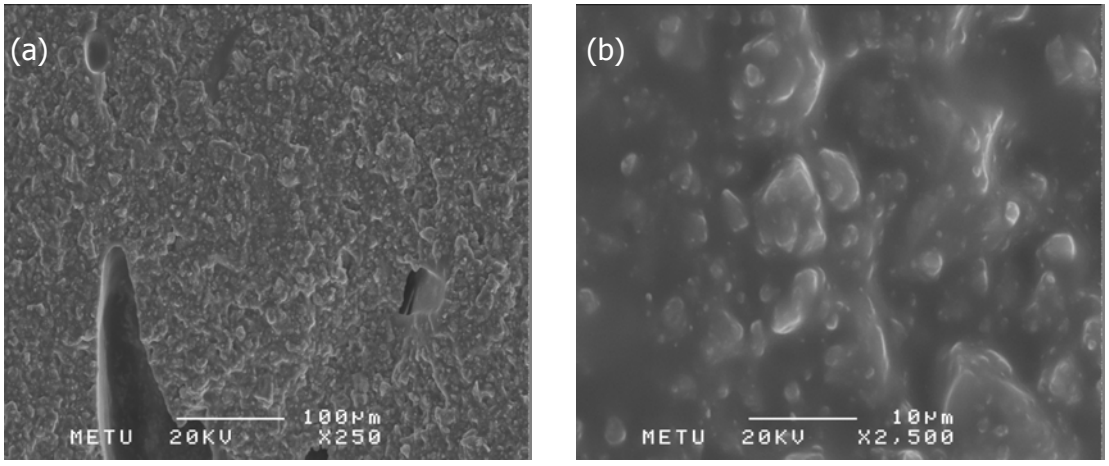

Figure 4.8 SEM micrographs of the material containing 5 vol. % EVA at (a) x250, (b) x2500 magnifications

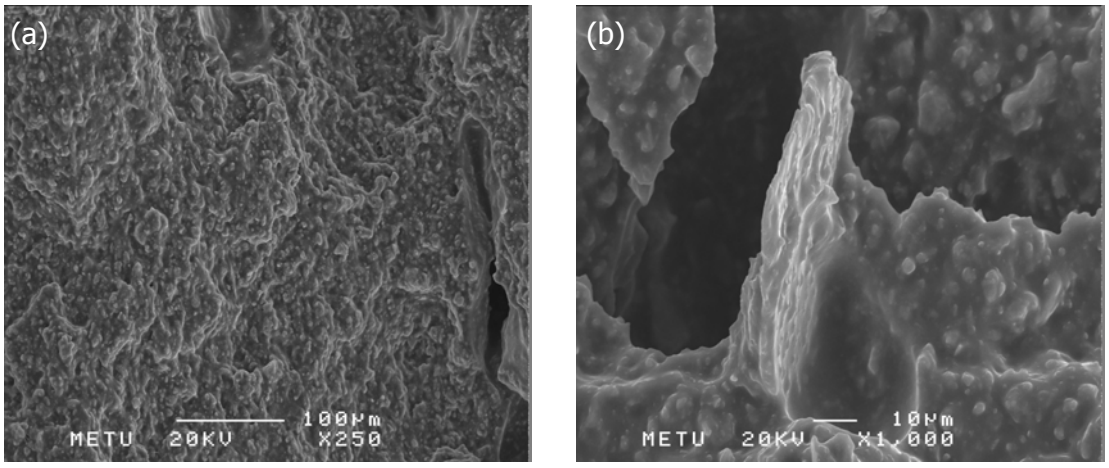

Figure 4.9 SEM micrographs of the material containing 6 vol. % SBS at (a) x250, (b) x2500 magnifications

4.2 Density Measurements

Density measurements of the specimens can be used in order to verify the existence of voids in composite structure. The deviations from theoretical densities are an indicator of void volume in the structure of bituminous composites.

Density measurements were performed with a densitometer. Theoretical density values are calculated from weight fractions for each sample. These results are summarized in Table 4.2 which includes materials that do not contain kieselguhr and in Table 4.3 that includes materials which contain various fractions of kieselguhr.

Table 4.2 Density measurements of samples do not contain kieselguhr

Sample No	Bitumen (20/30)	Bitumen (50/70)	$CaCO_3$	CaO	Baryte	Mica	EVA	SBR	SBS	density of sample (g/cm^3)	theoretical density (g/cm^3)
1	18.0	22.0	50.0	2.0	-	2.0	-	-	6.0	1.91	1.92
2	18.0	22.0	53.0	-	-	2.0	5.0	-	-	1.78	1.94
3	19.0	22.0	54.0	2.0	-	-	2.0	0.2	0.4	2.00	1.97
4	19.0	22.0	52.0	2.0	-	2.0	2.0	0.3	0.4	1.97	1.97
5	20.0	23.0	45.0	2.0	7.0	-	2.0	0.3	0.5	2.09	2.06
6	20.0	23.0	40.0	2.0	10.0	2.0	-	-	3.0	1.91	2.08
7	21.0	25.0	32.0	2.0	15.0	2.0	2.0	0.4	0.5	1.96	2.17
8	21.0	25.0	34.0	2.0	15.0	-	2.0	0.4	0.5	1.97	2.17
9	22.0	27.0	15.0	2.0	30.0	-	3.0	0.4	0.5	2.17	2.36
10	24.0	30.0	-	2.0	40.0	-	3.0	0.4	0.5	2.23	2.51

It is seen from Table 4.2 that, there is no significant difference between theoretical and experimental density values. Some bubble formation causes little differences in these measurements. The samples that contain baryte on the other hand show that measured density values are consistently less than theoretical densities and the difference in densities increases as baryte content increases. Baryte is also significantly porous, as given in Table 3.8, 14-16 g oil absorption for 100 g of baryte , so, about 30 % porosity exists in baryte which can result in partial impregnation with bitumen creating voids. Table 4.3 represents density results of kieselguhr containing materials. Density values of kieselguhr in each sample were calculated with the help of weight fractions and density measurements of samples (Calculations are given in Appendix).

Table 4.3 Density results of samples containing kieselguhr

Sample No	Bitumen (20/30)	Bitumen (50/70)	$CaCO_3$	CaO	Mica	Silaned Kieselguhr	Kieselguhr	density of sample (g/cm^3)	porosity of K.G. (%)	density of K.G. (g/cm^3)
11	20.0	24.0	44.0	2.0	2.0	-	5.0	1.91	31.37	1.85
12	-	50.0	40.0	-	-	-	10.0	1.77	31.48	1.85
13	22.0	26.0	33.0	2.0	-	-	15.0	1.73	52.74	1.28
14	-	50.0	30.0	-	-	-	20.0	1.69	32.96	1.81
15	-	50.0	40.0	-	-	10.0	-	1.77	28.30	1.94
16	17.0	21.0	45.0	2.0	2.0	10.0	-	1.86	64.07	0.97
17	22.0	27.0	34.0	2.0	-	15.0	-	1.66	64.81	0.95
18	-	50.0	30.0	-	-	20.0	-	1.66	28.89	1.92
19	16.0	19.0	38.0	2.0	2.0	20.0	-	1.89	41.19	1.59
21	16.0	19.0	36.0	2.0	2.0	25.0	-	1.85	41.11	1.59
22	16.0	19.0	35.0	2.0	-	25.0	-	1.80	51.52	1.31
23	16.0	19.0	35.0	2.0	-	25.0	-	1.80	48.93	1.32
24	-	50.0	20.0	-	-	30.0	-	1.54	29.63	1.90

It is observed from the Table 4.3 that, densities of both silaned and unmodified kieselguhr in materials which compose of 50 volume percent of 50/70 penetration bitumen are in the range of 1.80-1.95 g/cm^3. By comparison, these values are higher than that of 20 volume percent composition. This observation shows that, 50/70 penetration bitumen, because it is less viscous with respect to 20/30, permeates through pores inside of kieselguhr more easily. It should be noticed in Table 4.3 that, with viscous 20/30 bitumen a smaller fraction of the pores are filled with bitumen giving rise to a larger porosity value.

4.3 Porosity and Wetting of Kieselguhr

Kieselguhr (KG) powder is highly porous. Porosity may have various effects in terms of mechanical properties and thermal conduction when KG is used as filler in bitumen based composites. Partial impregnation of bitumen can increase the physical adhesion between the filler and the matrix that can result in improvement of mechanical properties. It is also expected to have lower thermal conduction due to the formation of air packets in KG powder.

The producers value of oil absorption into kieselguhr is given as 140 cm^3 oil per 100 g of KG. Taking a solid density of 2.70 g/cm^3 for KG gives 79.1 % porosity for KG powder assuming total impregnation of oil. Density measurements with pycnometer carried out on KG in water gave 2.625 g/cm^3 which indicates that water almost totally impregnates KG. On the other hand, density measurement on silaned kieselguhr (SKG) gave 0.352 g/cm^3 that shows that due to large contact angle on silaned surface water can not impregnate SKG powders. SKG actually floats on water so the porosity calculated from the above density is not reliable because of the formation of air pockets in between SKG particles on the surface. It can only be deduced that silane treatment makes KG totally impervious to water.

Impregnation studies are also carried out with dodecane on KG and SKG. With KG a density value of 2.313 g/cm^3 is found which implies that 14.3 % pore volume remains in KG and dodecane is capable of filling 85.7 % of the pores. With SKG in dodecane a porosity of 33.3 % is calculated. The impregnation of dodecane into SKG is reduced compared KG. Bitumen which is close to dodecane in chemical structure (both are basically hydrocarbons) can be expected to show similar behavior.

Another method to approximate the porosity of KG and SKG is by measuring the tapped density of the dry powders. It is known that the random packing of heterogeneous particles gives, depending of many functions, on the average 35 % porosity in between the powder particle [32]. The tapped density of KG and SKG is

measured in a volume calibrated container. By using 0.65 packing factor the porosity of KG is found as 79 %. It is interesting to note that, this value is very close to the one reported by the producer. SKG gave a porosity of 75.3 % under the same conditions. One can say that the silaning process decreases the pore size and pore volume slightly by getting adsorbed onto the capillary surfaces of KG.

In the light of studies made on KG and SKG with water and dodecane one can expect a partial impregnation of KG with bitumen and a still reduced amount of impregnation of bitumen in the case of SKG. The result of impregnation studies given above is summarized in Table 4.4. The solid density of KG is taken as 2.7 g/cm^3 and densities of dodecane and water are 0.75 and 0.9982 g/cm^3.

Table 4.4 Density and porosity results of KG and SKG from different experimental techniques

	density (g/cm³)	porosity (%)
Producer's value for KG	2.79	79.10
KG in water	2.63	76.60
SKG in water	0.35	87.00
KG in dodecane	2.31	14.30
SKG in dodecane	1.80	33.30
Tapped KG	0.37	79.00
Tapped SKG	0.43	75.30

The percent porosity values of kieselguhr in the composites were calculated from the density measurements and listed in Table 4.3. The value given for SKG in water is not reliable. From the table, one can deduce that silanation process reduces the pore volume to some extent (tapped KG and SKG values). On the average KG powder has a porosity of 77-79 % and the SKG has 75-76 % porosity.

4.3.1 Mercury Porosimeter results of Kieselguhr

Mercury porosimeter is capable of detecting pores which are larger than 1000 Å in diameter. Figure 4.10 gives the pore size distrubution of KG which is a binodal distribution. There are pores in the vicinity of 10000 Å and 100000 Å ranges. The overall porosity is calculated as 47.5 %. For SKG (Figure 4.11) the pore size distribution is uninodal with a mean of 5000 Å. The total porosity is 30 %. This result indicates that the silanation process, used in this study, blocks or decreases the sizes of the pores and reduces the percent porosity values. The silaned KG has smaller pore fraction compared to unmodified KG.

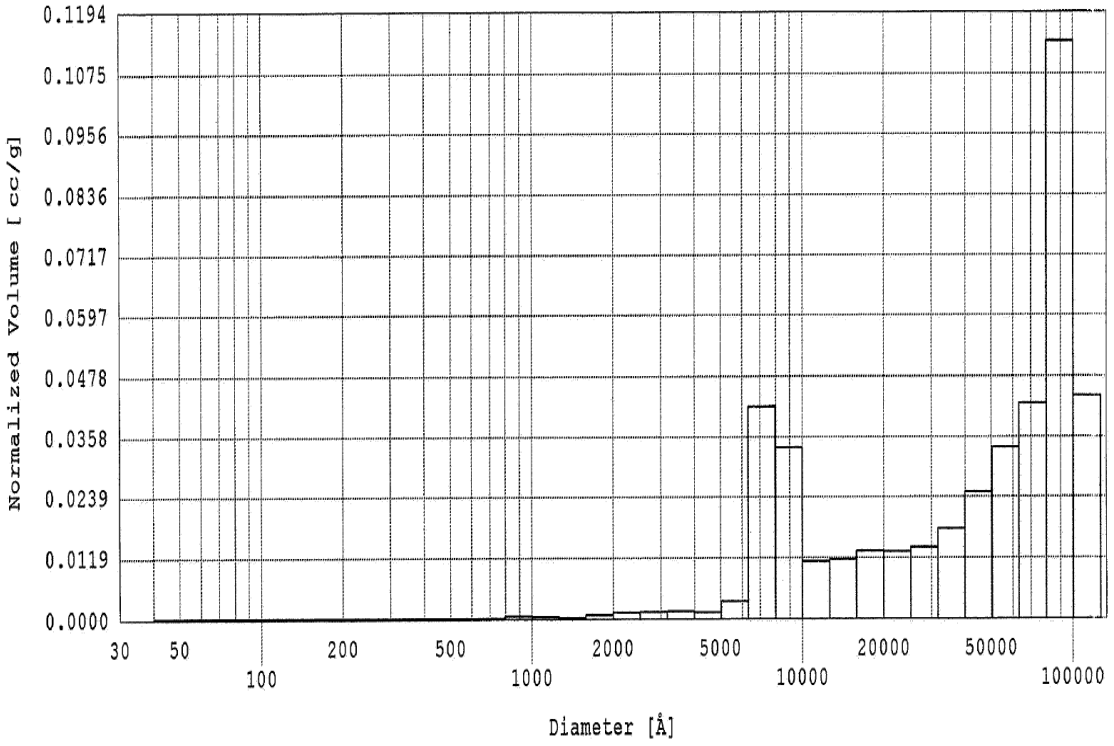

Figure 4.10 Pore size histogram of kieselguhr

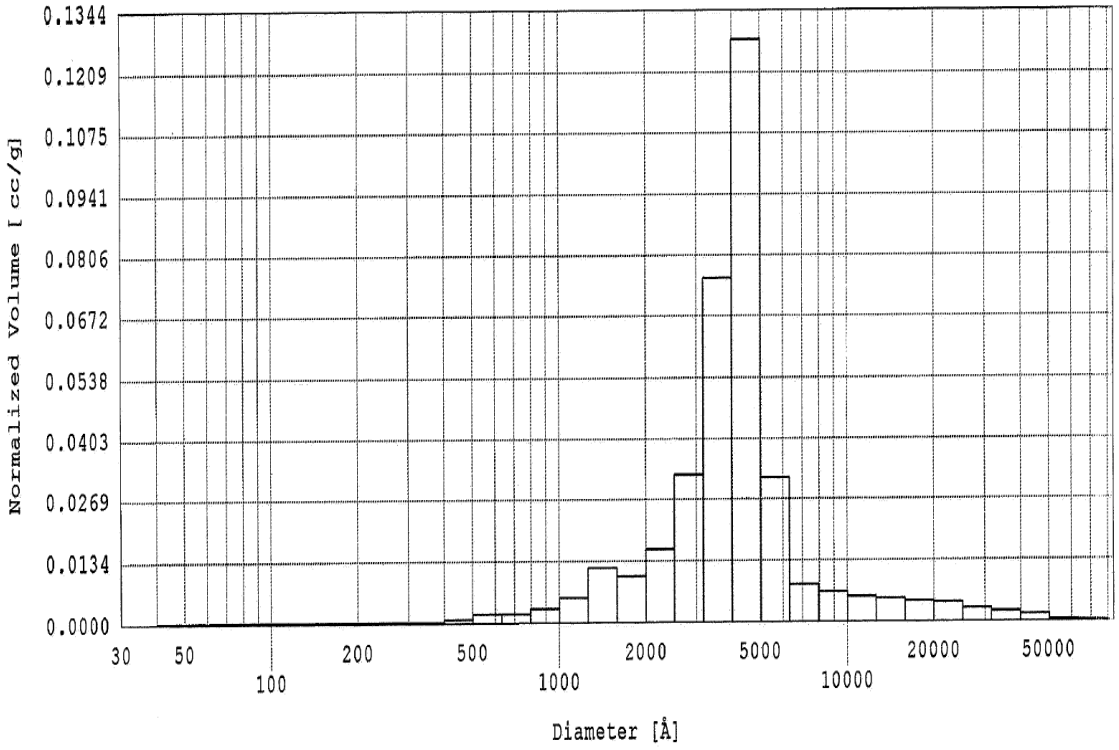

Figure 4.11 Pore size histogram of silaned kieselguhr

4.4 Flow Characteristics

4.4.1 Melt Flow Index Test (MFI)

Melt flow index test was applied to obtain information about flow characteristics of prepared bituminous materials. Test was performed under specified loads of 2.16 kg and 5 kg at 130 ^{0}C and 2.16 kg at 180 ^{0}C . Results were expressed in grams/10 min. Table 4.5 shows the compositions of samples in MFI tests.

Table 4.5 Volume percentages of samples in MFI tests

Sample No	Bitumen (20/30)	Bitumen (50/70)	$CaCO_3$	CaO	Baryte	Mica	Silaned Kieselguhr	Kieselguhr	MFI at 130 C^0 (2.16 kg)	MFI at 130 C^0 (5 kg)	MFI at 180 C^0 (2.16 kg)
3	19.0	22.0	54.0	2.0	-	-	-	-	4.8	19.2	74.3
4	19.0	22.0	52.0	2.0	-	2.0	-	-	8.4	34.5	136.0
5	20.0	23.0	45.0	2.0	7.0	-	-	-	22.8	100.2	83.2
7	21.0	25.0	32.0	2.0	15.0	2.0	-	-	26.5	97.7	84.7
8	21.0	25.0	34.0	2.0	15.0	-	-	-	0.2	1.0	0.2
9	22.0	27.0	15.0	2.0	30.0	-	-	-	48.9	277.2	379.4
10	24.0	30.0	-	2.0	40.0	-	-	-	93.4	392.4	696.0
12	-	50.0	40.0	-	-	-	-	10.0	22.2	42.6	105.4
14	-	50.0	20.0	-	-	-	-	20.0	1.0	2.0	4.4
15	-	50.0	40.0	-	-	-	10.0	-	134.1	220.6	-
18	-	50.0	30.0	-	-	-	20.0	-	202.0	348.0	-
24	-	50.0	20.0	-	-	-	30.0	-	260.0	528.0	-

In general, addition of baryte increases the MFI values. Mica also has a similar effect; as mica amount is increased from 0 % to 2 % a significant increase in MFI is observed. On the other hand, KG decreases MFI indicating the formation of a viscous material.

As seen in Figure 4.12, MFI values increase with addition of baryte. The effect is basically due to the extremely high density of baryte which facilitates the vertical sedimentation rate of the baryte powder in the MFI meter. Compared to $CaCO_3$, baryte is also poorly wetted by bitumen which gives rise to a weaker interaction between baryte and bitumen compared to $CaCO_3$ powder. At 30 % volume fraction an extremely high MFI value was recorded for baryte.

Figure 4.13 and 4.14 show the flow characteristics of mica containing samples. Materials at Figure 4.13 contain 15 % vol. baryte with 2 vol. % mica and without mica. At Figure 4.14 represents the material containing 2 vol. % mica and without mica and these samples contain about 50 % calcium carbonate instead of baryte. It is seen that, melt flow rates are slightly greater at Figure 4.13 than Figure 4.14, which confirms the previous discussion about baryte. There is another result concluded from both these figures that MFI values increase with addition of mica. It is seen from Figure 4.14, 2 vol. % addition of mica to the material resulted in an MFI value of about 60 g/10 min. at 180 ^{0}C. Plate-like structure of mica particles are oriented along the flow direction and result in increased MFI. The result is well-known for mica-like particles in laminar flow regimes. Orientation of particles decreases the viscosity during flow. The higher the flow rate is the smaller the viscosity gets.

Effect of Kieselguhr content on MFI is represented in Figure 4.15. These results are very different from that of baryte and mica. Fluidity of kieselguhr containing materials decreases sharply with addition of kieselguhr. It is observed that at 20 vol. %, melt flow rate is very close to zero. At mixing stage, bitumen molecules penetrate the pores inside KG and with addition high concentrations of filler, bitumen molecules fill these pores and reducing the amount of bitumen in the matrix. As a result, material obtains a highly viscous form and almost does not flow even at 180 ^{0}C.

In the case of surface-silaned kieselguhr, similar results to baryte and mica are determined as seen from Figure 4.16. MFI values increase proportionally with addition of silaned filler. Because of surface silanation made pores of kieselguhr stay unfilled, bitumen flows freely and interacts with only surface of the filler by weak bonds, so material gets softer and more sensitive to temperature. This is further evidence that through silanation process, the impregnation of bitumen into the pores of SKG is prevented to a large extent.

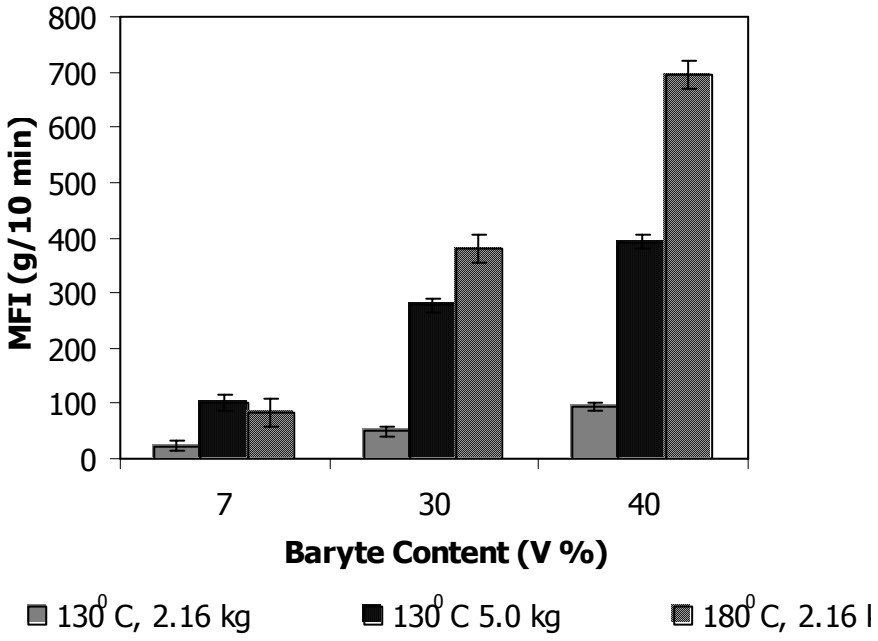

Figure 4.12 Effect of Baryte content on melt flow index

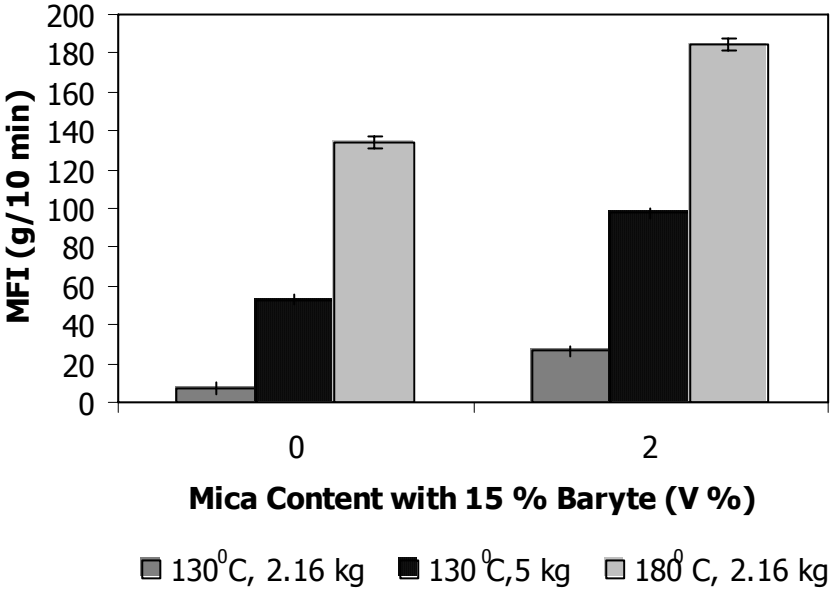

Figure 4.13 Effect of Mica content with a constant volume of Baryte on melt flow index

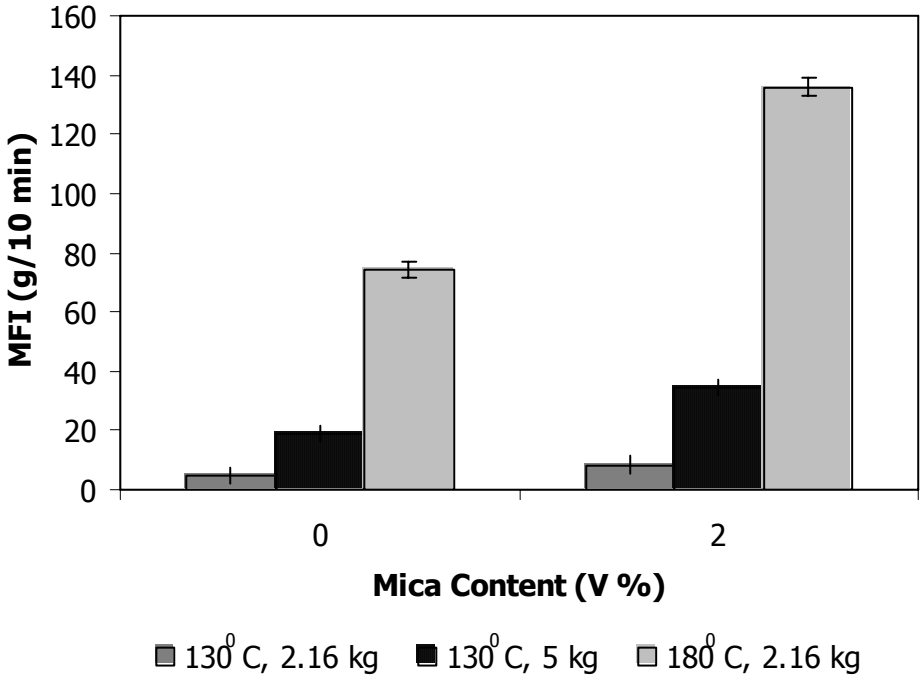

Figure 4.14 Effect of Mica content on melt flow index

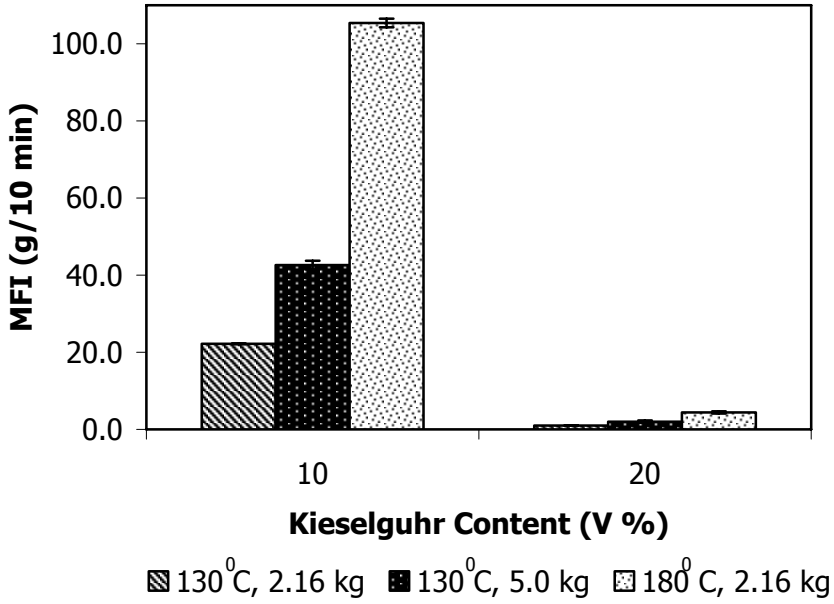

Figure 4.15 Effect of Kieselguhr content on melt flow index

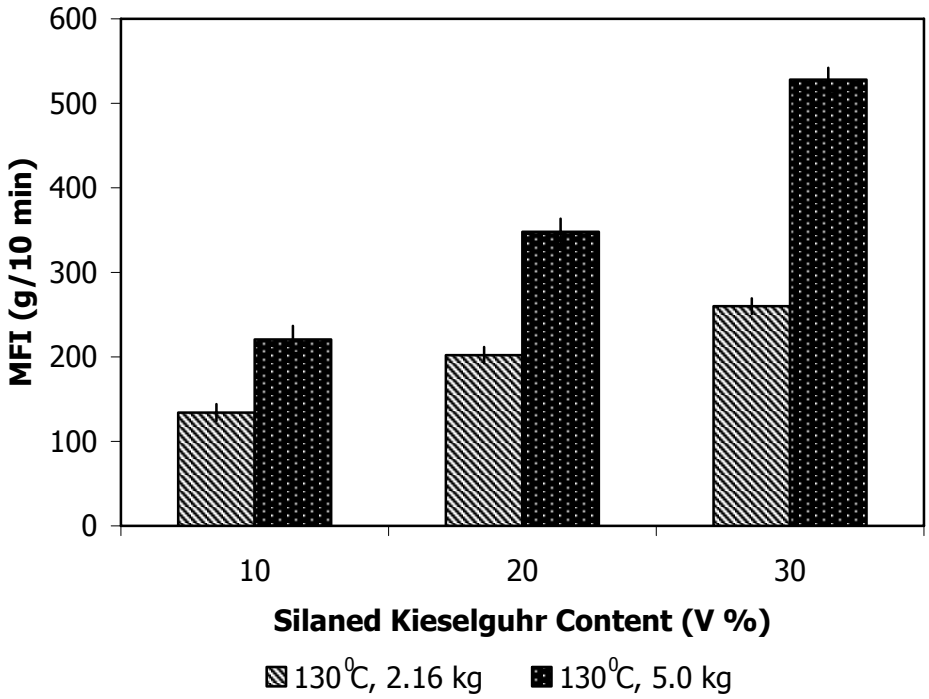

Figure 4.16 Effect of Silaned Kieselguhr content on melt flow index

4.5 Mechanical Tests

In this study, tensile tests are performed to examine the effect of different fillers and concentration on mechanical properties of the bituminous materials.

4.5.1 Tensile Test

The previous Table 3.15 summarizes all the mechanical tests carried out on bituminous composites. The results of the selected tests are given in Table 4.6 and Figure 4.17 through 4.21. Effect of baryte, kieselguhr and silaned kieselguhr to tensile

strength, percentage strain and Young's modulus are discussed with the help of tensile test results.

Table 4.6 Volume percentages of samples in tensile tests

Sample No	Bitumen (20/30)	Bitumen (50/70)	$CaCO_3$	CaO	Baryte	Mica	Silaned Kieselguhr	Kieselguhr	Max. Tensile Strength	Max. Percentage Strain
5	20.0	23.0	45.0	2.0	7.0	-	-	-	4.3	7.1
7	21.0	25.0	32.0	2.0	15.0	2.0	-	-	3.7	6.8
9	22.0	27.0	15.0	2.0	30.0	-	-	-	2.5	9.4
10	24.0	29.0	-	2.0	40.0	-	-	-	2.2	10.1
11	20.0	24.0	49.0	2.0	-	2.0	-	5.0	2.2	7.7
12	-	50.0	40.0	-	-	-	-	10.0	1.5	19.3
14	-	50.0	30.0	-	-	-	-	20.0	1.1	16.2
15	-	50.0	40.0	-	-	-	10.0	-	1.3	3.5
18	-	50.0	30.0	-	-	-	20.0	-	0.5	30.2
24	-	50.0	20.0	-	-	-	30.0	-	0.5	28.0

Mechanical properties of baryte containing samples were studied by tensile test results of baryte at 7, 15, 30, 40 vol. % concentrations. Young's modulus values of baryte containing samples are shown as a function of baryte content in Figure 4.17. It is seen that, Young's Modulus value of material which contains lowest baryte (7 vol. %) is greater than materials of higher baryte content and Young's modulus decreases sharply as the baryte content increases. The same trend is observed for tensile strength values of these materials. It is seen from the Figure 4.18 that, tensile strength is greatly influenced by the content of baryte and as the baryte content increases tensile strength decreases. This result probably is due to attractions of the polar molecules on bitumen to baryte molecules and decreasing calcium carbonate content. Another reason may be the porosity of baryte and the impregnation of

bitumen resulting in a decreased amount of bitumen acting as matrix element. Percentage strain at break values is reported in Figure 4.19. As seen from the figure, with addition of baryte, materials show sharp increase in percentage strain. Percentage strains of materials contain baryte with 30 and 40 volume % are close to each other.

Kieselguhr naturally has very porous structure (porosity from 65 to 85%) characterized by a system of numerous channels encapsulated in a perforated shell. For instance, it has the specialty of able to absorb high amounts of liquids. Its oil absorption varies in the range of 100-200g/100g [15]. With the help of surface silanation process, it was aimed to get kieselguhr remain porous. Silane molecules on the surface of kieselguhr prevent the penetration into the pores (shells) of kieselguhr during mixing process. From these predictions, it was expected that prepared bituminous materials would contain voids inside kieselguhr with the help of surface silanation process.

Materials contain KG prepared at three compositions (5, 10, 20 by volume) and for SKG at three concentrations (10, 20, 30 by volume). As a difference from the other specimens, polymers were not used in this case to see the effect of KG alone. Figure 4.20 demonstrates the effect of kieselguhr and silaned kieselguhr content on the tensile strength of the composites. It is apparent that, addition of both silaned and unmodified kieselguhr lowers the tensile strength of the material. Comparison of these two graphs gave conclusions about effect of silane modification on tensile strength of materials. It is seen from the figure that, surface silanation applied kieselguhr lowers the strength of material as compared with kieselguhr contained samples at 10 and 20 % by volume concentrations. As a result of penetration of bitumen molecules into pores of kieselguhr, binder-filler interactions are much stronger than that of silaned surfaces of kieselguhr, materials contained unmodified filler has greater tensile strength than modified one at the same concentrations. Percentage strain results are given in Figure 4.21. The same trend is observed in both kieselguhr types that is,

addition of filler leads to higher strain value, but with further addition of filler resulted in slightly decreasing in percentage strain.

If one turns back to Table 3.15, among of the samples tested, the optimum configuration of the ingredients which are mechanically strong with acceptable strain values and at the same time has good thermal isolation character can be deducted. In samples with KG sample 13 and with SKG sample 23 look very promising. In samples with no kieselguhr sample 7 and sample 9 are good candidates depending on the property one wants to maximize.

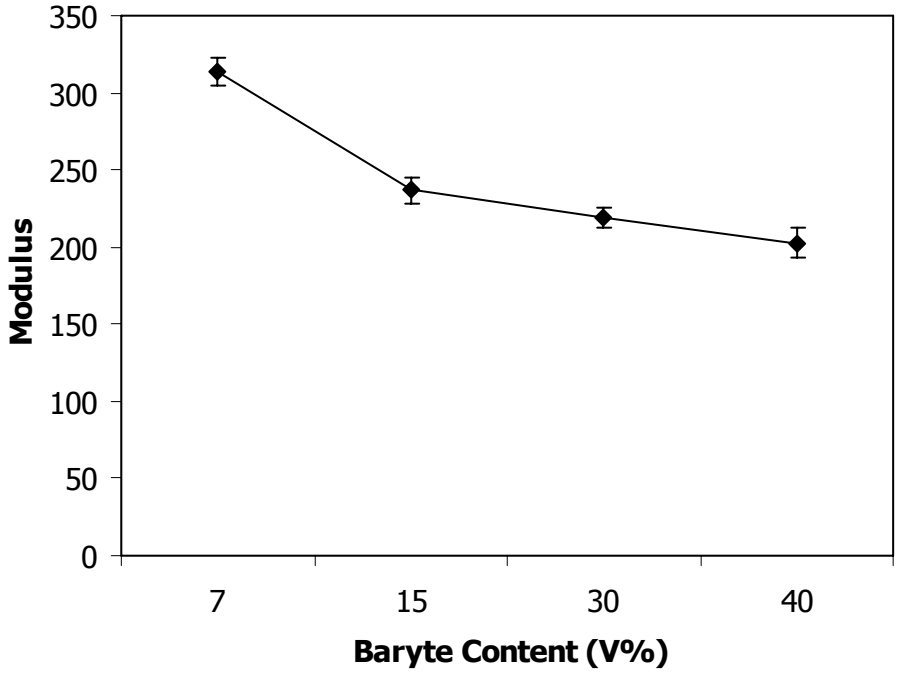

Figure 4.17 Effect of Baryte Content on Young's Modulus

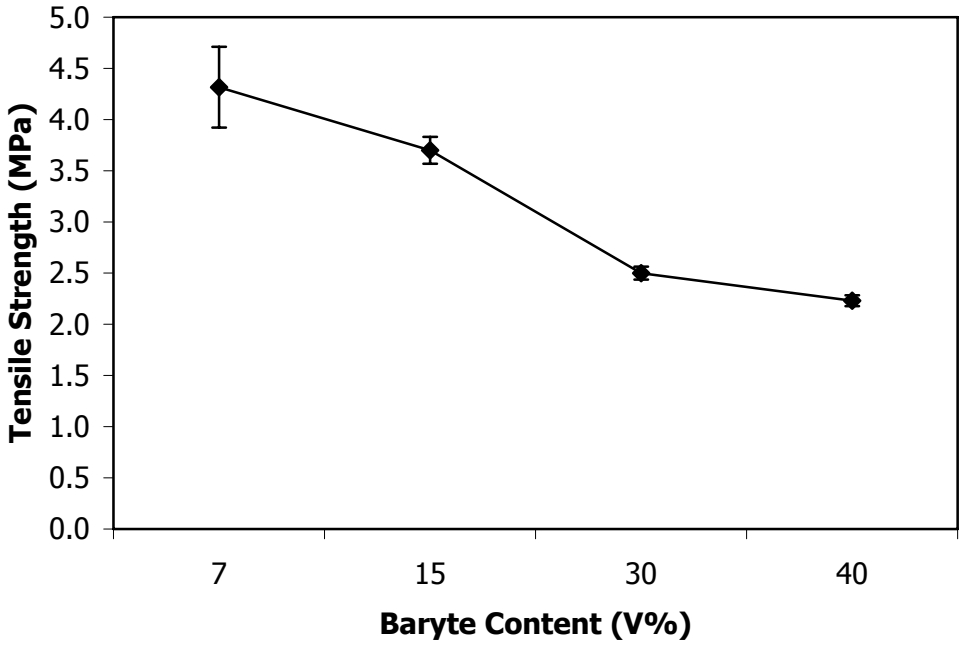

Figure 4.18 Effect of Baryte content on Tensile Strength

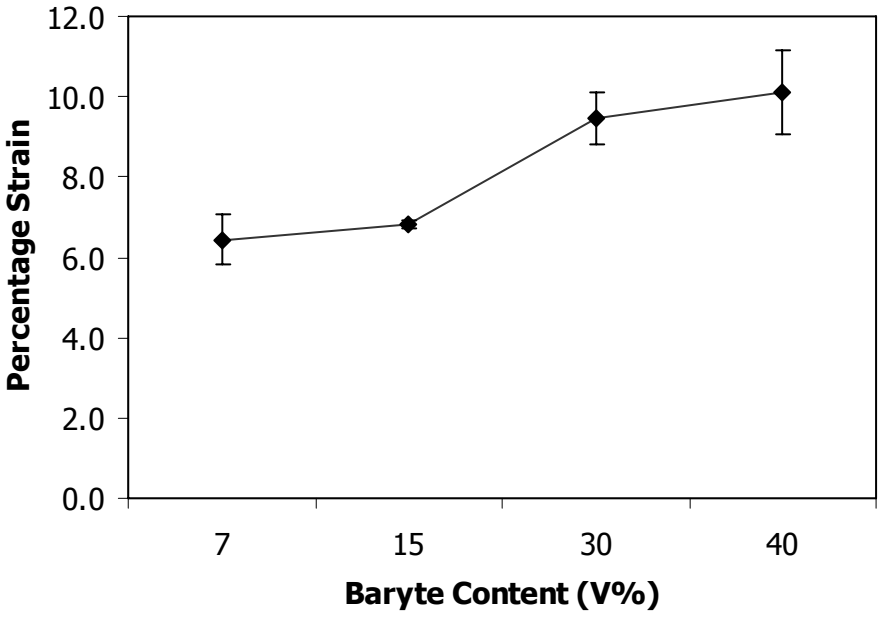

Figure 4.19 Effect of Baryte content on Percentage Strain

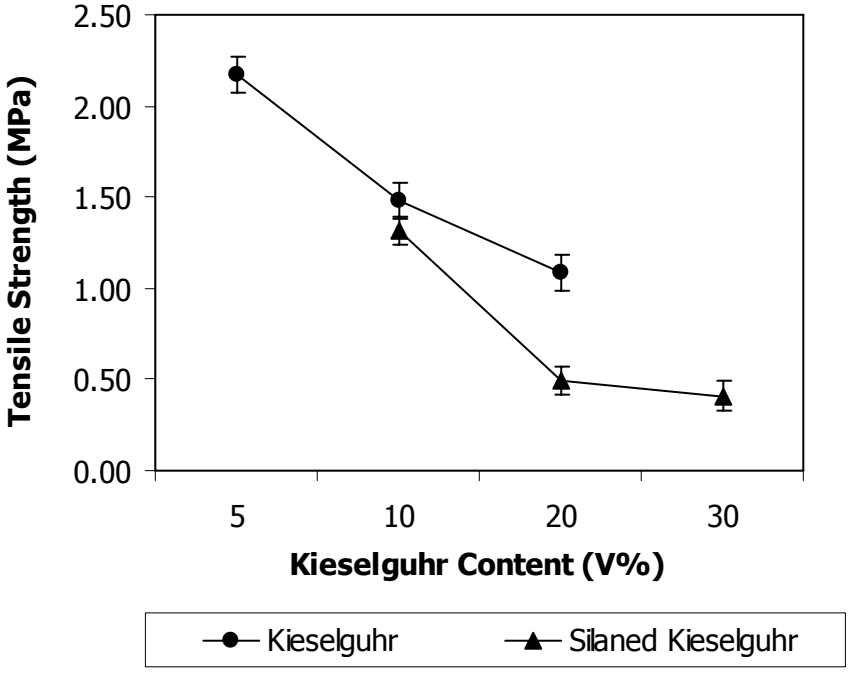

Figure 4.20 Effect of Kieselguhr and Silaned Kieselguhr content on Tensile strength

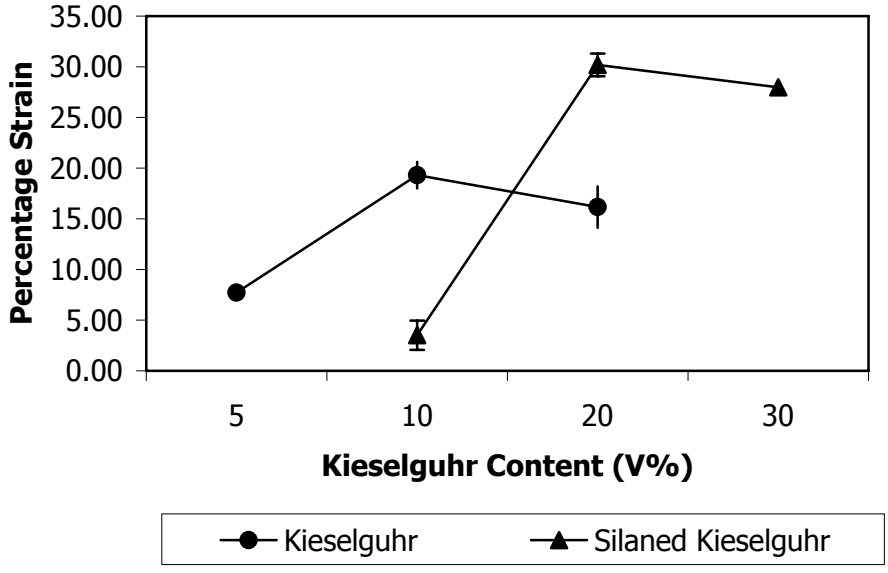

Figure 4.21 Effect of Kieselguhr and Silaned Kieselguhr content on Percentage Strain

4.6 Thermal Tests

4.6.1 Thermal Conductivity Test

Hot wire method was used for thermal measurements of prepared samples. Effect of filler type and ratio to thermal behavior was examined. Test results are given in Table 4.7 and discussed in terms of thermal isolation capacity.

Table 4.7 Thermal conductivity results of materials according to volume percents of fillers

Sample No	Bitumen (20/30)	Bitumen (50/70)	$CaCO_3$	CaO	Baryte	Mica	Silaned Kieselguhr	Kieselguhr	Conductivity (W/m.K)
6	20.0	23.0	40.0	2.0	10.0	2.0	-	-	0.80
7	21.0	25.0	32.0	2.0	15.0	2.0	-	-	0.77
9	22.0	27.0	15.0	2.0	30.0	-	-	-	0.59
11	20.0	24.0	44.0	2.0	-	2.0	-	5.0	0.89
13	22.0	26.0	33.0	2.0	-	-	-	15.0	0.92
16	17.0	21.0	45.0	2.0	-	2.0	10.0	-	0.97
17	22.0	27.0	34.0	2.0	-	-	15.0	-	0.74
19	16.0	19.0	38.0	2.0	-	2.0	20.0	-	0.86
20	19.0	22.0	31.0	2.0	6.0	-	20.0	-	0.78
21	16.0	19.0	36.0	2.0	-	2.0	25.0	-	0.86
22	16.0	19.0	35.0	2.0	-	-	25.0	-	0.87
23	16.0	19.0	35.0	2.0	-	-	25.0	-	0.88

From Table 4.7, it is clearly observed that baryte containing samples have smaller thermal conductivity values and addition of baryte lowers the conductivity. At 30 vol. % concentration, value of 0.59 W/m.K is obtained which is very low conductivity as

compared with that of all the samples in table. From sharp decrease at 30 vol. % sample represented in Figure 4.22, it is concluded that, bituminous materials that containing large amounts of baryte are effective in thermal isolation basically due to high heat capacity of baryte.

It is clearly seen from the Table 4.7 that, unmodified kieselguhr is not suitable for heat isolation of bituminous materials as expected. It is predicted that, unfilled pores inside kieselguhr absorb and isolate heat that flows through material. For this reason, surface of kieselguhr was coated with silanes and migration of the bitumen phase into the pores was prevented. Thermal conductivity results show that, these expectations come true experimentally; silaned kieselguhr containing samples have lower conductivity values as compared to that of kieselguhr.

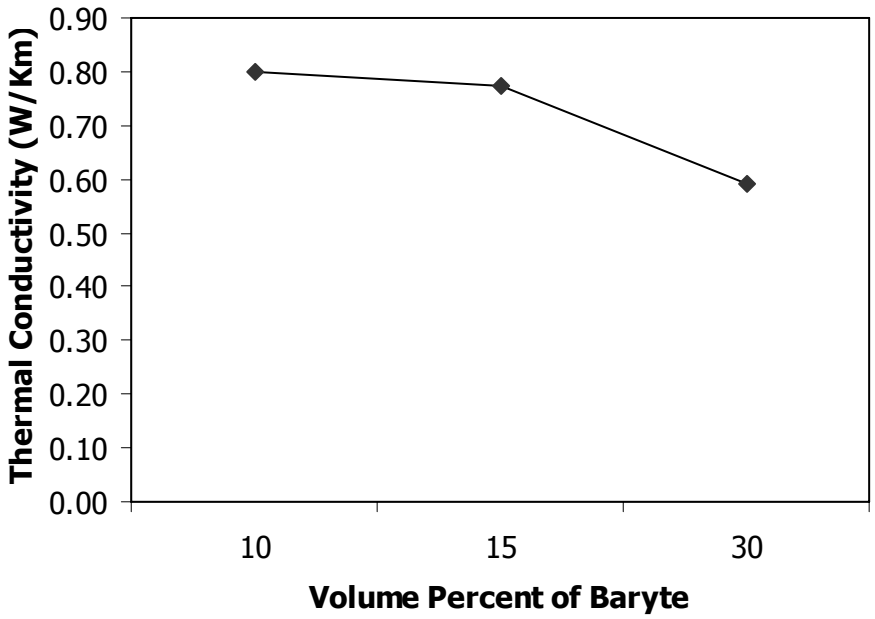

Figure 4.22 Effect of Baryte content on Thermal Conductivity

CHAPTER V

CONCLUSIONS

In this study, we attempted to find the effects of various fillers on the mechanical, rheological and thermal properties of bitumen based composites. Among the fillers $CaCO_3$ is the basic one due to its cost and availability and CaO because of its hydroscopic properties. Mica, when used at low percentages has the effect of decreasing the viscosity of the bitumen due to its flow alignment property. Baryte was used in order to make use of its high heat capacity and low heat conductivity. The effects of both of these two fillers are verified through MFI and heat conductivity measurements.

Polymers are also used in order to increase the mechanical properties of the composites. EVA containing samples showed the best combination of tensile strength and percent elongation.

Another aim of the study was to improve the heat resistivity (decrease heat conductivity) of the bituminous composite to obtain a material with good mechanical and heat isolation properties. KG and SKG are used in order to make use of the porus structure of these materials. To control the amount of bitumen that impregnates the KG powder, surface silanation is applied on KG creating a non-wetting surface and pore structure. The silanation process decreased the pore sizes as observed in mercury porosimetry experiments. A decreased amount of bitumen impregnation is obtained by the silanation process, clearly observed in SEM micrographs.

In conclusion, valuable information is obtained in order to design a bituminous composite material that has superior mechanical and thermal isolation properties. The functions and related parameters of the various fillers used in this study are elucidated.

REFERENCES

1. John M. Bostwick, "Industrial Minerals and Rocks (Nonmetallics other than Fuels)", 4th Edition, American institute of Mining, Metallurgical, and Petroleum Engineers, Applied Clay Science, Vol. 15, 11-29, 1999.

2. Arnold J. Hoiberg, "Bituminous Materials, Asphalts", Tars, Pitches, Vol. 1, John Willey & Sons, Inc. , 348, 1964.

3. O. Gonzalez, M.E. Munoz, A. Santamaria , M. Garcia-Morales, F.J. Navarro, P. Partal, "Rheology and stability of bitumen/EVA blends", European Polymer Journal, Vol. 40, 2004.

4. http://www.petroleumbazaar.com/Bitumen/bitappli.htm, last accesed, December 2006.

5. The Columbia Encyclopedia, Sixth Edition, Columbia University Press, 2005.

6. Peterson J.C., TRB 63rd Meeting, Washington, Halstead, W.J. Proc AAPT, Vol. 54, 1985.

7. V. Selvavathi, Vijai ArunSekar, V. Sairam, B. Sairam, "Modification of Bitumen By Elastomer And Reactive Polymer—A Comparative Study", Petroleum Science And Technology, Vol. 20 (5&6), 535–547, 2002.

8. http://www.slurry.com/techpapers/techpapers_contrbit.shtml, last accesed, December 2006.

9. http://www.responseonline.com, last accesed, December 2006.

10. Perez-Lepe A., Martinez-Boza F.J., Gallegosa C., Gonzalez O., Munoz M.E., Santamaria A., "Influence of the processing conditions on the rheological behaviour of polymer-modified bitumen", Fuel, Vol. 82, 1339-1348, 2003.

11. Lu X., Isacsson U., "Influence of styrene-butadiene-styrene polymer modification on bitumen viscosity", Fuel, Vol. 76, 1353-1359, 1997.

12. M. García-Morales, P. Partal, F.J. Navarro, F.J. Martínez-Boza, C. Gallegos, "Rheology of Recycled EVA Modified Bitumen", Annual European Rheology Conference 2003, Guimarães–Portugal, 2003.

13. Traxler R.N., "Asphalt Its Compositions, Properties and Uses", Reinhold Publishing Corporation, Newyork, 1961.

14. William C. Wake, "Fillers for Plastics", Iliffe for the Plastics Institute, 1971.

15. Wypych, Jerzy, "Fillers", Chem Tech Publishing, Toronto, 1993.

16. http://www.gov.ns.ca/natr/meb/pdf/90egs01/90egs01_Chapter01.pdf, last accesed, December 2006.

17. Xanthos M., "Functional Fillers for Plastics", Wiley-Vch Verlag GmbH & Co. KgaA, Weinheim, 2005.

18. Shah, Vishu, "Handbook of Plastic Testing Technology", Second Edition, A Wiley-Interscience Publication, 1998.

19. http://www.tpl.ukf.sk/engl_vers/hot_wire.htm, last accesed, December 2006.

20. Chris Rauwendaal, "Polymer Mixing: A Self-Study Guide", Hanser Publishers, Munich, 1998.

21. Fritschy G., Papirer E., "Interactions between a bitumen, its components and model fillers", Fuel, Vol. 57, 701-704, 1978.

22. Craus J., Ishai I., Por N., "Selective sorption in filler-bitumen systems", Journal of Materials Science, Vol. 14, No. 9 , 2195 – 2204, 1979.

23. Dubey S.T., Waxman M.H., "Asphaltene Adsorption and Desorption from Mineral Surfaces", SPE Reservoir Engineering Journal, 389-395, 1995.

24. L.S. Johansson, U. Isacsson, "Effect of filler on low temperature physical hardening of bitumen", Construction and Building Materials, Vol. 12, 463-470, 1998.

25. M.F.C. Van de Ven and K. Jenkins, "Rheological characterisation of some (polymer modified) bitumen and bitumen-filler system at compaction and in-service temperatures", 6th RILEM Symposium PTEBM, Zurich, 2003.

26. K. Baginska, I. Gawel, "Effect of origin and technology on the chemical composition and colloidal stability of bitumens", Fuel Processing Technology, Vol. 85, 1453–1462, 2004.

27. Dallas N. Little, J. Claine Petersen, "Unique Effects of Hydrated Lime Filler on the Performance-Related Properties of Asphalt Cements: Physical and Chemical Interactions Revisited", Journal of Materials in Civil Engineering, Vol. 17, No. 2, 207-218, 2005.

28. Karaşahin M., Terzi S., "Evaluation of marble waste dust in the mixture of asphaltic concrete", Construction and Building Materials, in press, 2006.

29. Annual Book of ASTM Standards, Vol. 08.01, American Society for Testing and Materials, ASTM D638-91a, Philadelphia, USA, 1993.

30. http://www.kampus.tse.org.tr/EN/kimyacer.asp, last accesed, December 2006.

31. Lu X., Isacsson U., "Modification of road bitumens with thermoplastic polymers", Polymer Testing, Vol. 20, 77–86, 2001.

32. Gray W.A., "The Packing of Solid Particles", Chapman and Hall, London, 1968.

APPENDIX

DENSITY AND POROSITY CALCULATIONS

General expression for 100 g kieselguhr:

$$\frac{\text{weight of bitumen}}{\text{density of bitumen}} + \frac{\text{weight of } CaCO_3}{\text{density of } CaCO_3} + \frac{\text{weight of CaO}}{\text{density of CaO}} + \frac{\text{weight of mica}}{\text{density of mica}} + \frac{\text{weight of KG}}{\text{density of KG}} + \frac{\text{weight of SBS}}{\text{density of SBS}} + \frac{\text{weight of EVA}}{\text{density of EVA}} = \frac{100\text{ g material}}{\text{density of material}}$$

$$\%\text{ porosity} = 1 - \frac{\text{density of KG}}{2.7\text{ g/cm}^3} \times 100$$

Sample 11:

$$\frac{20.9\text{g bitumen}}{1.0\text{g/cm}^3} + \frac{63.4\text{ g } CaCO_3}{2.71\text{g/cm}^3} + \frac{3.8\text{ g CaO}}{3.34\text{g/cm}^3} + \frac{2.4\text{ g mica}}{2.8\text{g/cm}^3} + \frac{8\text{ g KG}}{\text{density of KG}} + \frac{1.5\text{ g SBS}}{0.9\text{g/cm}^3} = \frac{100\text{g material}}{1.913\text{g/cm}^3}$$

density of KG=1.853 g/cm^3

$$\%\text{ porosity} = 1 - \frac{1.853\text{ g/cm}^3}{2.7\text{ g/cm}^3} \times 100 = 31.37\ \%$$

Sample 12:

$$\frac{27.0\text{ g bitumen}}{1.0\text{g/cm}^3} + \frac{56.7\text{ g } CaCO_3}{2.71\text{g/cm}^3} + \frac{14.3\text{ g KG}}{\text{density of KG}} = \frac{100\text{g material}}{1.773\text{g/cm}^3}$$

density of KG=1.850 g/cm^3

$$\%\text{ porosity} = 1 - \frac{1.850\text{ g/cm}^3}{2.7\text{ g/cm}^3} \times 100 = 31.48\ \%$$

Sample 13:

$$\frac{20.9\text{g bitumen}}{1.0\text{g/cm}^3}+\frac{56.4\text{ g CaCO}_3}{2.71\text{g/cm}^3}+\frac{3.8\text{ g CaO}}{3.34\text{g/cm}^3}$$
$$+\frac{17.5\text{ g KG}}{\text{density of KG}}+\frac{1.0\text{ g EVA}}{0.94\text{g/cm}^3}+\frac{0.2\text{ g SBS}}{0.9\text{ g/cm}^3}=\frac{100\text{g material}}{1.730\text{g/cm}^3}$$

density of KG=1.276 g/cm^3

$$\%\text{ porosity}=1-\frac{1.276\text{ g/cm}^3}{2.7\text{ g/cm}^3}\times 100=52.74\ \%$$

Sample 14:

$$\frac{27.0\text{ g bitumen}}{1.0\text{g/cm}^3}+\frac{44.5\text{ g CaCO}_3}{2.71\text{g/cm}^3}+\frac{28.5\text{ g KG}}{\text{density of KG}}=\frac{100\text{g material}}{1.691\text{g/cm}^3}$$

density of KG=1.810 g/cm^3

$$\%\text{ porosity}=1-\frac{1.810\text{ g/cm}^3}{2.7\text{ g/cm}^3}\times 100=32.96\ \%$$

sample 15:

$$\frac{30.0\text{ g bitumen}}{1.0\text{g/cm}^3}+\frac{65.7\text{ g CaCO}_3}{2.71\text{g/cm}^3}+\frac{4.3\text{ g KG}}{\text{density of KG}}=\frac{100\text{g material}}{2.22\text{g/cm}^3}$$

density of KG=1.936 g/cm^3

$$\%\text{ porosity}=1-\frac{1.936\text{ g/cm}^3}{2.7\text{ g/cm}^3}\times 100=28.30\ \%$$

Sample 16:

$$\frac{20.9\text{g bitumen}}{1.0\text{g/cm}^3}+\frac{67.4\text{ g CaCO}_3}{2.71\text{g/cm}^3}+\frac{3.8\text{ g CaO}}{3.34\text{g/cm}^3}$$
$$+\frac{2.4\text{ g mica}}{2.8\text{g/cm}^3}+\frac{4\text{ g KG}}{\text{density of KG}}+\frac{1.5\text{ g SBS}}{0.9\text{g/cm}^3}=\frac{100\text{g material}}{1.864\text{g/cm}^3}$$

density of KG=0.951 g/cm^3

$$\%\text{ porosity}=1-\frac{0.951\text{ g/cm}^3}{2.7\text{ g/cm}^3}\times 100=64.07\ \%$$

Sample 17:

$$\frac{28.0\text{g bitumen}}{1.0\text{g/cm}^3}+\frac{57.69\text{ g CaCO}_3}{2.71\text{g/cm}^3}+\frac{3.5\text{ g CaO}}{3.34\text{g/cm}^3}$$
$$+\frac{2.18\text{ g mica}}{2.8\text{g/cm}^3}+\frac{7.28\text{ g KG}}{\text{density of KG}}+\frac{1.4\text{ g SBS}}{0.9\text{g/cm}^3}=\frac{100\text{g material}}{1.657\text{g/cm}^3}$$

density of KG=0.950 g/cm^3

$$\%\text{ porosity}=1-\frac{0.950\text{ g/cm}^3}{2.7\text{ g/cm}^3}\times 100=64.81\ \%$$

Sample 18:

$$\frac{34.7\text{ g bitumen}}{1.0\text{g/cm}^3}+\frac{55.3\text{ g CaCO}_3}{2.71\text{g/cm}^3}+\frac{10.0\text{ g KG}}{\text{density of KG}}=\frac{100\text{g material}}{1.658\text{g/cm}^3}$$

density of KG=1.920 g/cm^3

$$\%\text{ porosity}=1-\frac{1.920\text{ g/cm}^3}{2.7\text{ g/cm}^3}\times 100=28.89\ \%$$

sample 19:

$$\frac{20.9\text{g bitumen}}{1.0\text{g/cm}^3}+\frac{63.4\text{ g CaCO}_3}{2.71\text{g/cm}^3}+\frac{3.8\text{ g CaO}}{3.34\text{g/cm}^3}$$
$$+\frac{2.4\text{ g mica}}{2.8\text{g/cm}^3}+\frac{8.0\text{ g KG}}{\text{density of KG}}+\frac{1.5\text{ g SBS}}{0.9\text{g/cm}^3}=\frac{100\text{g material}}{1.887\text{g/cm}^3}$$

density of KG=1.588 g/cm^3

$$\%\text{ porosity}=1-\frac{1.588\text{ g/cm}}{2.7\text{ g/cm}^3}\times 100=41.19\ \%$$

Sample 21:

$$\frac{20.9\text{g bitumen}}{1.0\text{g/cm}^3}+\frac{59.4\text{ g CaCO}_3}{2.71\text{g/cm}^3}+\frac{3.8\text{ g CaO}}{3.34\text{g/cm}^3}$$
$$+\frac{2.4\text{ g mica}}{2.8\text{g/cm}^3}+\frac{12.0\text{ g KG}}{\text{density of KG}}+\frac{1.5\text{ g SBS}}{0.9\text{g/cm}^3}=\frac{100\text{g material}}{1.851\text{g/cm}^3}$$

density of KG=1.590 g/cm^3

$$\%\ \text{porosity} = 1 - \frac{1.590\ \text{g/cm}^3}{2.7\ \text{g/cm}^3} \times 100 = 41.11\ \%$$

Sample 22:

$$\frac{20.9\text{g bitumen}}{1.0\text{g/cm}^3} + \frac{61.8\ \text{g CaCO}_3}{2.71\text{g/cm}^3} + \frac{3.8\ \text{g CaO}}{3.34\text{g/cm}^3} + \frac{12.0\ \text{g KG}}{\text{density of KG}} + \frac{1.5\ \text{g SBS}}{0.9\text{g/cm}^3} = \frac{100\text{g material}}{1.80\text{g/cm}^3}$$

density of KG=1.309 g/cm^3

$$\%\ \text{porosity} = 1 - \frac{1.309\ \text{g/cm}^3}{2.7\ \text{g/cm}^3} \times 100 = 51.52\ \%$$

Sample 23:

$$\frac{20.9\text{g bitumen}}{1.0\text{g/cm}^3} + \frac{59.4\ \text{g CaCO}_3}{2.71\text{g/cm}^3} + \frac{3.8\ \text{g CaO}}{3.34\text{g/cm}^3} + \frac{2.4\ \text{g mica}}{2.8\text{g/cm}^3} + \frac{12.0\ \text{g KG}}{\text{density of KG}} + \frac{1.5\ \text{g SBS}}{0.9\text{g/cm}^3} = \frac{100\text{g material}}{1.802\text{g/cm}^3}$$

density of KG=1.321 g/cm^3

$$\%\ \text{porosity} = 1 - \frac{1.321\ \text{g/cm}^3}{2.7\ \text{g/cm}^3} \times 100 = 48.93\ \%$$

Sample 24:

$$\frac{40.0\ \text{g bitumen}}{1.0\text{g/cm}^3} + \frac{42.8\ \text{g CaCO}_3}{2.71\text{g/cm}^3} + \frac{17.2\ \text{g KG}}{\text{density of KG}} = \frac{100\text{g material}}{1.542\text{g/cm}^3}$$

density of KG=1.900 g/cm^3

$$\%\ \text{porosity} = 1 - \frac{1.321\ \text{g/cm}^3}{2.7\ \text{g/cm}^3} \times 100 = 29.63\ \%$$